AWARD NUMBER: W81XWH-17-1-0470

TITLE: Targeted Lung-Derived Proteins as a Therapeutic Strategy Against Breast Cancer Metastasis

PRINCIPAL INVESTIGATOR: Dr. Alison Allan

CONTRACTING ORGANIZATION: The University of Western Ontario

REPORT DATE: September 2020

TYPE OF REPORT: Annual

PREPARED FOR: U.S. Army Medical Research and Development Command
Fort Detrick, Maryland 21702-5012

REPORT DOCUMENTATION PAGE

Form Approved
OMB No. 0704-0188

1. REPORT DATE	**2. REPORT TYPE**	**3. DATES COVERED**
Sept 2020	Annual	15 Aug 2019 – 14 Aug 2020

4. TITLE AND SUBTITLE
Targeting Lung-Derived Proteins as a Therapeutic Strategy Against Breast Cancer Metastasis

5a. CONTRACT NUMBER

5b. GRANT NUMBER
W81XWH-17-1-0470

5c. PROGRAM ELEMENT NUMBER

6. AUTHOR(S)
Dr. Alison Allan, Dr. Raimar Loebenberg

E-Mail: alison.allan@lhsc.on.ca

5d. PROJECT NUMBER

5e. TASK NUMBER

5f. WORK UNIT NUMBER

7. PERFORMING ORGANIZATION NAME(S) AND ADDRESS(ES)

THE UNIVERSITY OF WESTERN ONTARIO
1151 RICHMOND ST
LONDON ON CANADA N6A 5B8

8. PERFORMING ORGANIZATION REPORT NUMBER

9. SPONSORING / MONITORING AGENCY NAME(S) AND ADDRESS(ES)

U.S. Army Medical Research and Development Command
Fort Detrick, Maryland 21702-5012

10. SPONSOR/MONITOR'S ACRONYM(S)

11. SPONSOR/MONITOR'S REPORT NUMBER(S)

12. DISTRIBUTION / AVAILABILITY STATEMENT

Approved for Public Release; Distribution Unlimited

13. SUPPLEMENTARY NOTES

14. ABSTRACT

Therapy for lung metastasis is often given systemically, causing significant toxicity. However, the lung holds potential for direct targeting via inhaled drugs; an approach that has shown promise in treating respiratory diseases but remains underexplored in oncology. This project is testing the hypothesis that CD44-interacting proteins produced in the lung promote breast cancer metastasis and can be targeted directly using inhalable drug delivery. To date, the major findings for the project are that the CD44-interacting proteins OPN, FGF2, and E/P/L selectins have complementary and important roles in mediating breast cancer metastatic behavior in response to the lung microenvironment. OPN and selectins (but not FGF2) were found to be necessary for metastatic colonization of the lung, particularly for more aggressive breast cancer cell lines. The pan-selectin antagonist bimosiamose has been selected for further study and subjected to drug formulation, optimization and quality assurance into an inhalable inhibitor. Due to COVID19-related research shutdowns experienced between March-July 2020, a 12-month no cost extension was requested and granted. Research activities have now resumed, with in vivo pre-clinical therapeutic studies initiated and planned for completion by the end of the final year of the award.

15. SUBJECT TERMS

Breast cancer, metastasis, lung microenvironment, CD44, osteopontin (OPN), basic fibroblast growth factor (FGF2), E-selectin, L-selectin, P-selectin, nanoparticles, inhalable drug delivery, pre-clinical models

16. SECURITY CLASSIFICATION OF:			**17. LIMITATION OF ABSTRACT**	**18. NUMBER OF PAGES**	**19a. NAME OF RESPONSIBLE PERSON**
					USAMRMC
a. REPORT	**b. ABSTRACT**	**c. THIS PAGE**			**19b. TELEPHONE NUMBER** *(include area code)*
Unclassified	Unclassified	Unclassified	Unclassified	60	

TABLE OF CONTENTS

1. INTRODUCTION:

The lung is one of the most common and deadly sites of breast cancer metastasis, particularly in patients with aggressive triple-negative (TN) disease. Therapy for metastasis is often given systemically, causing significant toxicity. However, the lung (unlike other metastatic sites) holds potential for direct targeting via inhaled drugs; an approach that has shown promise in treating respiratory diseases but remains underexplored in oncology. We have previously developed inhalable drug-loaded nanoparticles for cancer, and in the current project we aim to apply this innovation in combination with novel biological targets to address the problem of breast cancer metastasis to lung. We have previously reported that the lung microenvironment promotes metastasis of breast cancer cells, particularly those with high expression of the cell-surface receptor CD44. In order to identify therapeutic targets in the lung, we have used novel *ex vivo* models and observed that the lung secretes several CD44-interacting proteins involved with metastasis, including osteopontin (OPN), E-,L-, P-selectins, and basic fibroblast growth factor (FGF2). The purpose of this project is to test the ***hypothesis*** that CD44-interacting proteins produced in the lung promote breast cancer metastasis and can be targeted directly using inhalable drug delivery. Specific Aim 1 involves elucidation of the mechanisms by which lung-derived OPN, E-,L-,P-selectins and FGF2 promote breast cancer metastasis to the lung. To assess this, we are using a 2D *ex vivo* model system involving conditioned media (CM) from murine lung, as well as a 3D *ex vivo* pulmonary metastasis assay (PuMA). These assays are being used in combination with human TN breast cancer cell lines and primary cells from patient-derived xenografts. Lung-derived proteins are being depleted from lung-CM using functional antibodies or by using lungs from specific knockout mice. Specific Aim 2 involves assessing the therapeutic potential of directly targeting CD44-interacting proteins in the lung. Antibodies or chemical inhibitors targeting OPN, FGF2, or selectins are being loaded into polybutyl cyanoacrylate nanoparticles and incorporated into inhalable effervescent carrier particles. Pre-clinical *in vivo* metastasis models will be combined with inhalable drug delivery to target the lung directly rather than systemically. Mice will be subjected treatment with inhibitor targeting the most promising lung-derived protein from Specific Aim 1. Both preventative (before metastasis occurs) and therapeutic (after metastases are established) regimens will be tested for their ability to reduce metastatic burden.

2. KEYWORDS:

Breast cancer, metastasis, lung microenvironment, CD44, osteopontin (OPN), basic fibroblast growth factor (FGF2), E-selectin, L-selectin, P-selectin, nanoparticles, inhalable drug delivery, pre-clinical models

3. ACCOMPLISHMENTS:

➢ What were the major goals of the project?

Table 1 lists the major goals of the project as stated in the approved SOW for the project, including the milestones/target dates and actual completion dates or (if not completed) the percentage of completion to date. **Major Goals** in **blue font** represent those that remain in progress to be completed in the final year of the grant.

Table 1: *Major goals of the project as stated in the approved SOW for the project*

Major Task/Goal	Milestones	Target Date for Milestone Completion	Actual Completion Date or % Completion
Major Task 1: *In vitro* assessment of distinct metastatic behaviors & mechanisms	• HRPO/ACURO determination/approval • Characterization of the *in vitro* functional and mechanistic influence of lung-derived CD44-interacting proteins on breast cancer metastatic behavior	August 2018	100% completed
Major Task 2: 3D *ex vivo* assessment of essential lung-derived factors	• Establishment of breeding colonies of knockout mice • Characterization of the essentiality of each lung-derived factor for breast cancer metastasis. • Generation of a priority list of lung-derived factors for Major Task 4 & 5.	August 2019	100% completed
Major Task 3: Formulation and production of inhalable inhibitors	• Successful formulation, production and QC/QA of an inhalable drug ready for use in first *in vivo* studies	February 2019	100% completed
Major Task 4: *In vivo* assessment of anti-metastatic efficacy of inhalable drug using a preventative approach	• *In vivo* testing of inhalable inhibitor in the preventative setting.	December 2019	10% completed
Major Task 5: *In vivo* assessment of anti-metastatic efficacy of inhalable drug using a therapeutic approach	• *In vivo* testing of inhalable inhibitor in the therapeutic setting. • Identification of lead candidate for future translation.	August 2020	0% completed
Major Task 6: Integrated data sharing plan between sites		Ongoing throughout whole funding period	Ongoing throughout whole funding period

➢ What was accomplished under these goals?

Major Task 1: ***In vitro* assessment of distinct metastatic behaviors & mechanisms.**

The proposed work for Major Task is complete and is described below. This work supported ***Specific Aim 1***, which was to determine the mechanisms by which lung-derived OPN, selectins and FGF2 support and promote breast cancer metastasis to the lung.

TASK 1.1: *Local IRB/IACUC Approval*; and TASK 1.2: *HRPO/ACURO Approval*.

This task has been completed as proposed. Local IACUC approval for all animal experiments in this study was achieved on February 08, 2017. USAMRMC Animal Care and Use Review Office (ACURO) approval was granted on March 02, 2017, and has been successful with continuing annual renewal of approval since then. Local IRB determination and exemption was completed on April 07, 2017 and sent to the HRPO for review. On June 21, 2017 the HRPO confirmed that the research activities within the project do not involve human subjects, and that the research may proceed with no further requirement for review by the HRPO.

TASK 1.3: *Generate lung-conditioned media (CM) for rescue and signaling experiments*.

This task has been completed as proposed. Lung-CM has either been used for Task 1.4 (described below), or has been banked at -80°C for use in future project-related research activities.

TASK 1.4: *Characterize the functional and mechanistic influence of lung-derived CD44-interacting proteins on breast cancer metastatic behavior*.

This task has been essentially completed as proposed, with an overview of the methodology shown in ***Figure 1***. Briefly, lung-CM from Task 1.3 was collected from *ex vivo* lung culture, and blocking/neutralizing antibodies against osteopontin (OPN), E-,L-, and P-selectins or FGF2 were used to immunodeplete each protein from lung-CM. Companion ELISA kits were used to quantify the presence of each protein in lung-CM and the extent of immunodepletion. Native and immunodepleted lung-CM was then used to assess (a) the functional effects of specific lung-derived CD44-interacting proteins on *in vitro* breast cancer metastatic behavior and (b) the influence on intracellular signaling.

Figures 2-6 ("A" panels) demonstrate that all 5 proteins are present in lung-CM and can be effectively immunodepleted. The functional effects of these lung-derived CD44-interacting proteins on *in vitro* breast cancer metastatic behavior were then examined using a selection of different human triple-negative (TN) breast cancer cell lines and specialized cell culture assays. As demonstrated in ***Figures 2-6***, each lung-derived CD44-interacting protein examined appears to have a distinct but complementary role in supporting and promoting breast cancer metastatic behavior in the lung microenvironment. For example, OPN is involved in both migration and growth (***Figure 2***); FGF2 is only involved in growth (***Figure 3***); and E-, L-, and P-selectins are only involved in migration (***Figures 4-6***). Importantly, the specificity of each lung-derived protein at influencing specific cell behaviors was confirmed by rescue experiments that involved adding recombinant OPN, FGF2, or selectins back to depleted lung-CM at concentrations equivalent to the original depletion. These results were also highly reproducible in different TN human breast cancer cell models including MDA-MB-231 and SUM-149 immortalized cell lines, and the LRCP-BR17 cells (derived from a TN patient-derived xenograft model).

To assess the differential activation of downstream signaling in breast cancer cells in response to lung-CM, we used a combination of protein phospho-array analysis (for broad

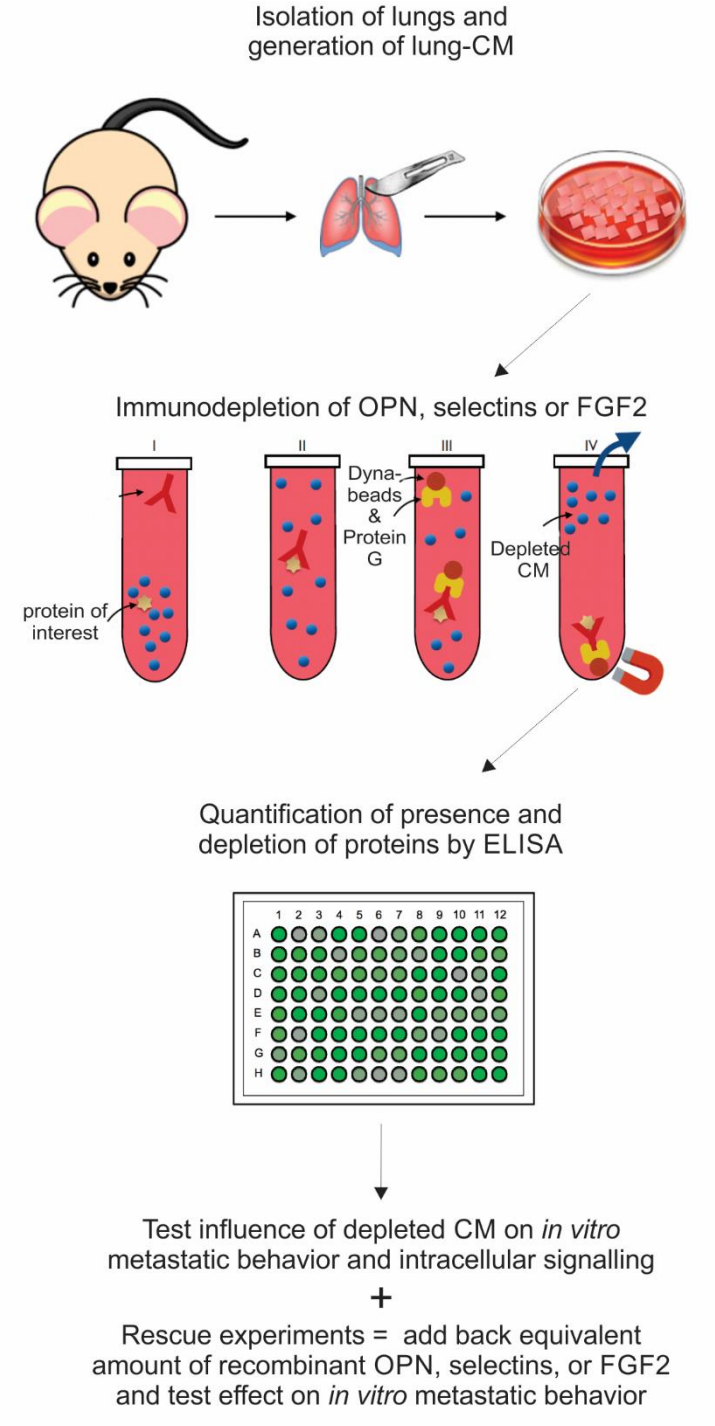

Figure 1: *Methodology overview for Major Task 1.*

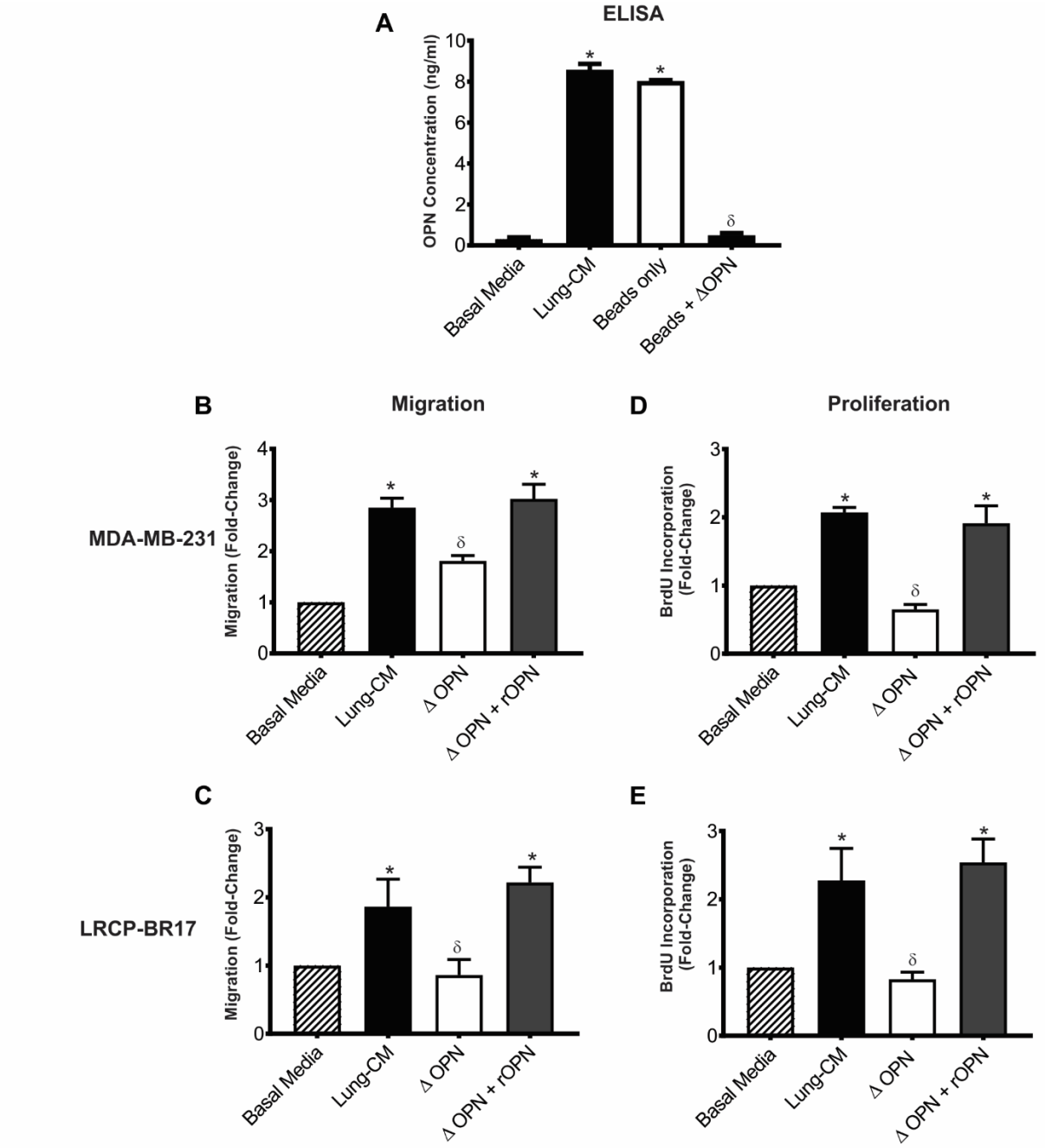

Figure 2: *Depletion of osteopontin (OPN) from lung conditioned media (CM) reduces breast cancer cell migration and proliferation*. **(A)** Lung-CM was generated from healthy female mouse lungs and OPN immunodepleted. Resulting OPN protein levels were determined by ELISA. Data are presented as mean [OPN] ± SEM (n = 3). **(B,C)** MDA-MB-231 and LRCP-BR17 cell migration following exposure to basal media, native lung-CM, lung-CM depleted of OPN (ΔOPN), or ΔOPN rescued by re-addition of recombinant OPN. **(D,E)** LRCP-BR17 cell proliferation following exposure to basal media, native lung-CM, lung-CM depleted of OPN (ΔOPN), or ΔOPN rescued by re-addition of recombinant OPN. Data are presented as mean fold-change in migration or BrdU incorporation relative to basal media ± SEM (n = 3). * = significantly different than basal media; δ = significantly different than native lung-CM ($p \leq 0.05$).

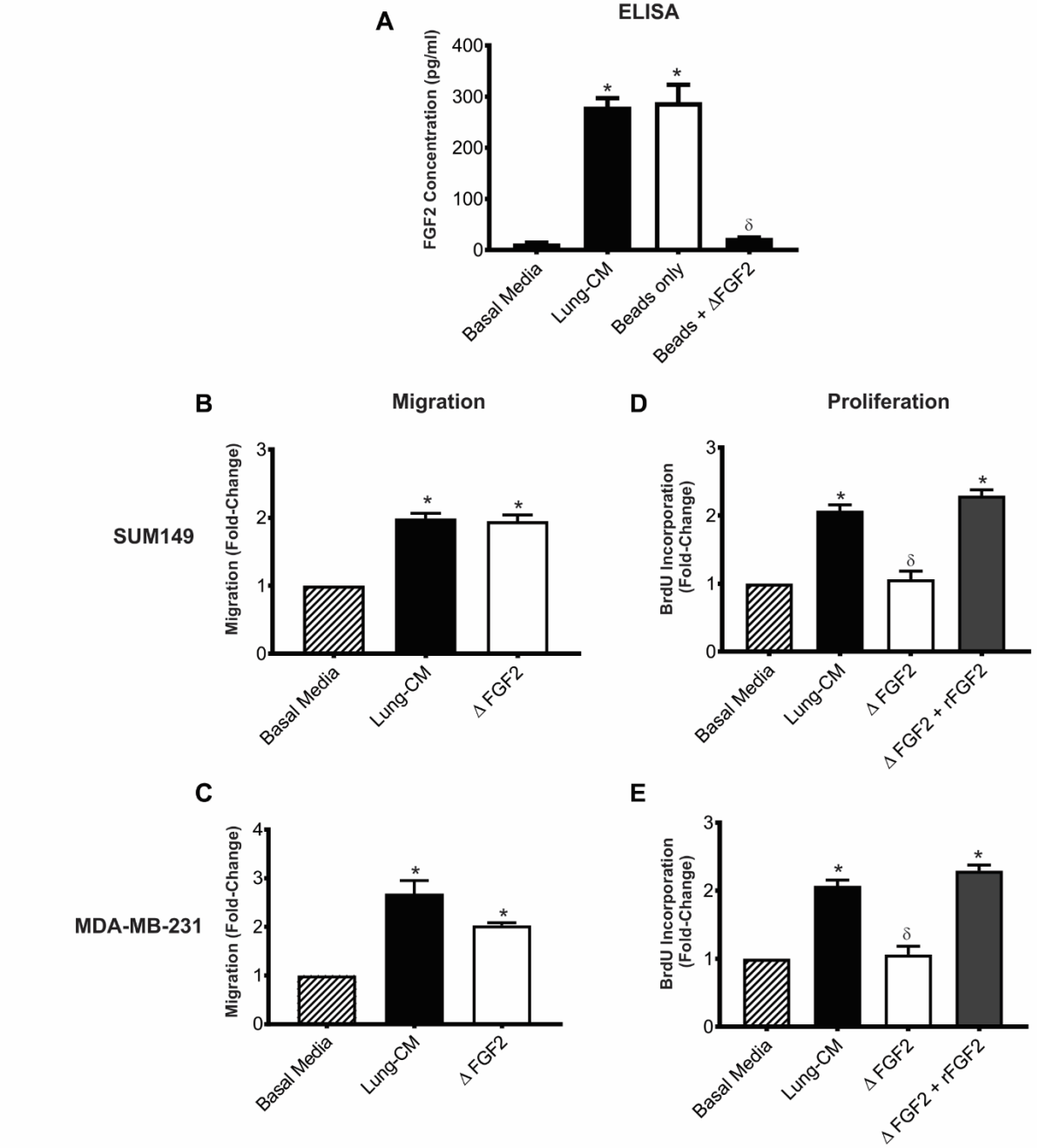

Figure 3: *Depletion of basic fibroblast growth factor (FGF2) from lung conditioned media (CM) reduces breast cancer cell proliferation but not migration*. **(A)** Lung-CM was generated from healthy female mouse lungs and FGF2 immunodepleted. Resulting FGF2 protein levels were determined by ELISA. Data are presented as mean [FGF2] ± SEM (n = 3). **(B,C)** SUM149 and MDA-MB-231 cell migration following exposure to basal media, native lung-CM, or lung-CM depleted of FGF2 (ΔFGF2). **(D,E)** SUM149 and MDA-MB-231 cell proliferation following exposure to basal media, native lung-CM, lung-CM depleted of FGF2 (ΔFGF2), or ΔFGF2 rescued by re-addition of recombinant FGF2. Data are presented as mean fold-change in migration or BrdU incorporation relative to basal media ± SEM (n = 3). * = significantly different than basal media; δ = significantly different than native lung-CM ($p \leq 0.05$).

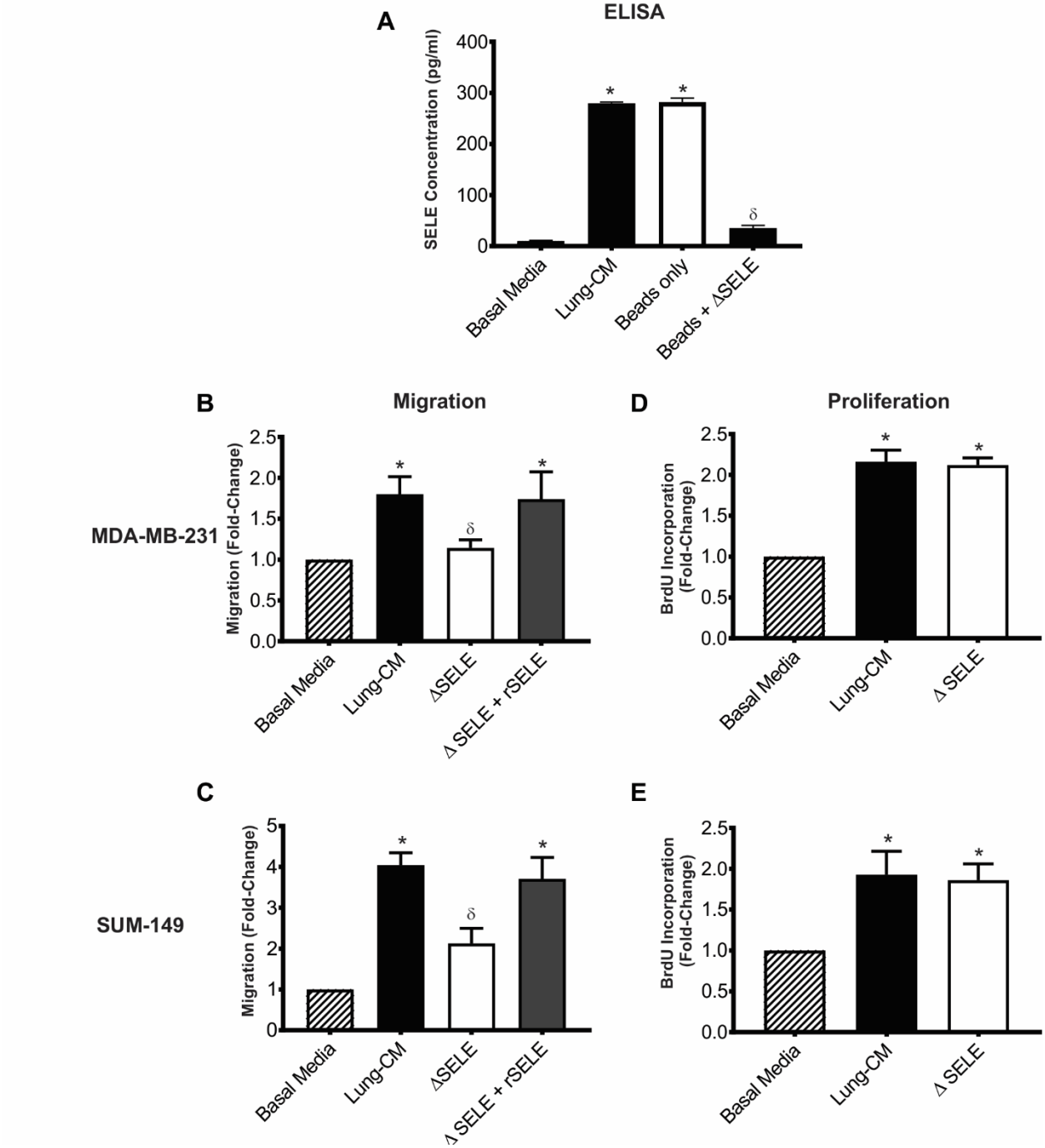

Figure 4: *Depletion of E-selectin (SELE) from lung conditioned media (CM) reduces breast cancer cell migration but not proliferation*. **(A)** Lung-CM was generated from healthy female mouse lungs and SELE immunodepleted. Resulting SELE protein levels were determined by ELISA. Data are presented as mean [SELE] ± SEM (n = 3). **(B,C)** MDA-MB-231 and SUM149 cell migration following exposure to basal media, native lung-CM, lung-CM depleted of SELE (ΔSELE), or ΔSELE rescued by re-addition of recombinant SELE. **(D,E)** MDA-MB-231 and SUM149 cell proliferation following exposure to basal media, native lung-CM, or lung-CM depleted of SELE (ΔSELE). Data are presented as mean fold-change in migration or BrdU incorporation relative to basal media ± SEM (n = 3). * = significantly different than basal media; δ = significantly different than native lung-CM ($p \leq 0.05$).

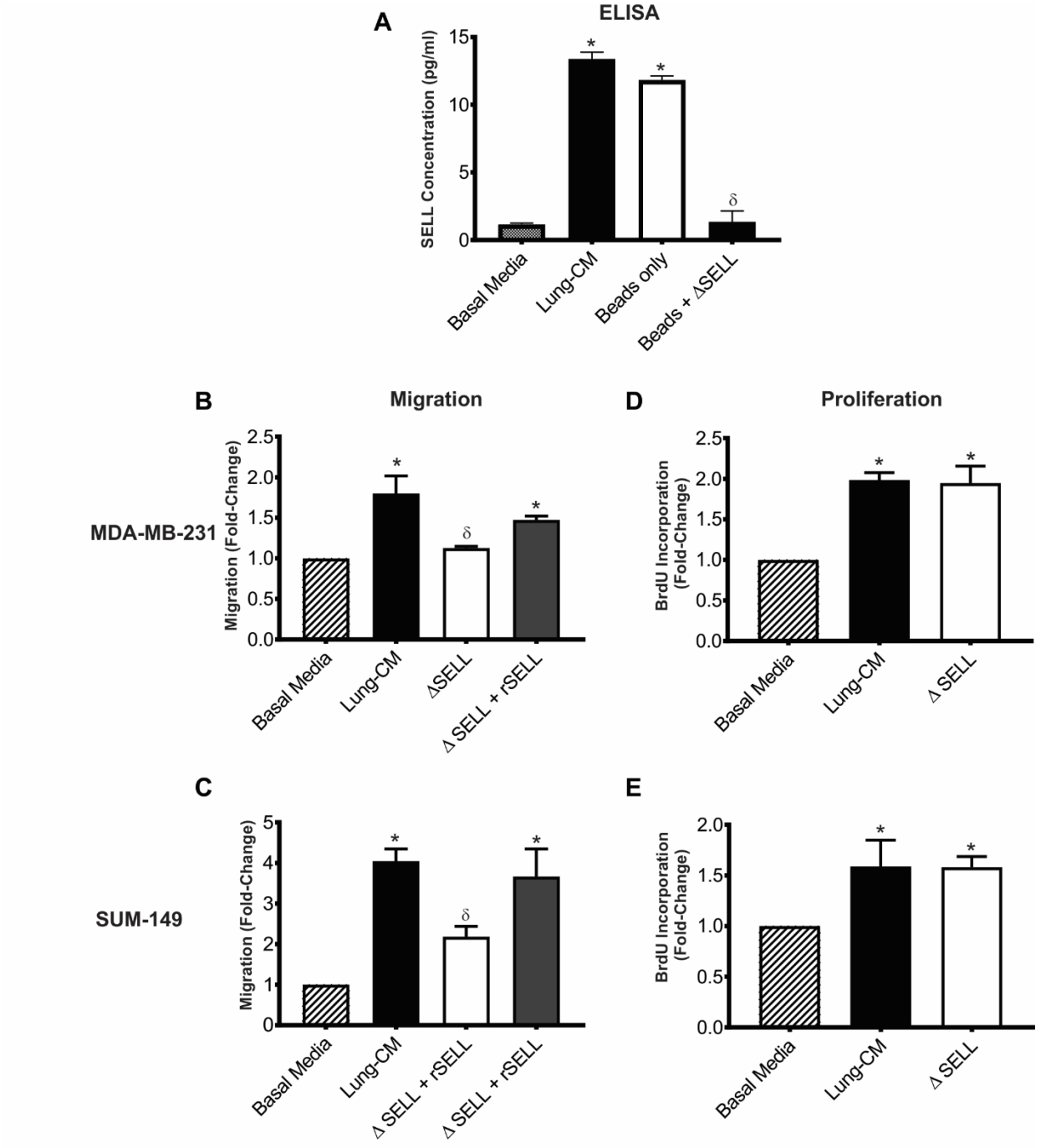

Figure 5: *Depletion of L-selectin (SELL) from lung conditioned media (CM) reduces breast cancer cell migration but not proliferation*. **(A)** Lung-CM was generated from healthy female mouse lungs and SELL immunodepleted. Resulting SELL protein levels were determined by ELISA. Data are presented as mean [SELL] ± SEM (n = 3). **(B,C)** MDA-MB-231 and SUM149 cell migration following exposure to basal media, native lung-CM, lung-CM depleted of SELL (ΔSELL), or ΔSELL rescued by re-addition of recombinant SELL. **(D,E)** MDA-MB-231 and SUM149 cell proliferation following exposure to basal media, native lung-CM, or lung-CM depleted of SELL (ΔSELL). Data are presented as mean fold-change in migration or BrdU incorporation relative to basal media ± SEM (n = 3). * = significantly different than basal media; δ = significantly different than native lung-CM ($p \leq 0.05$).

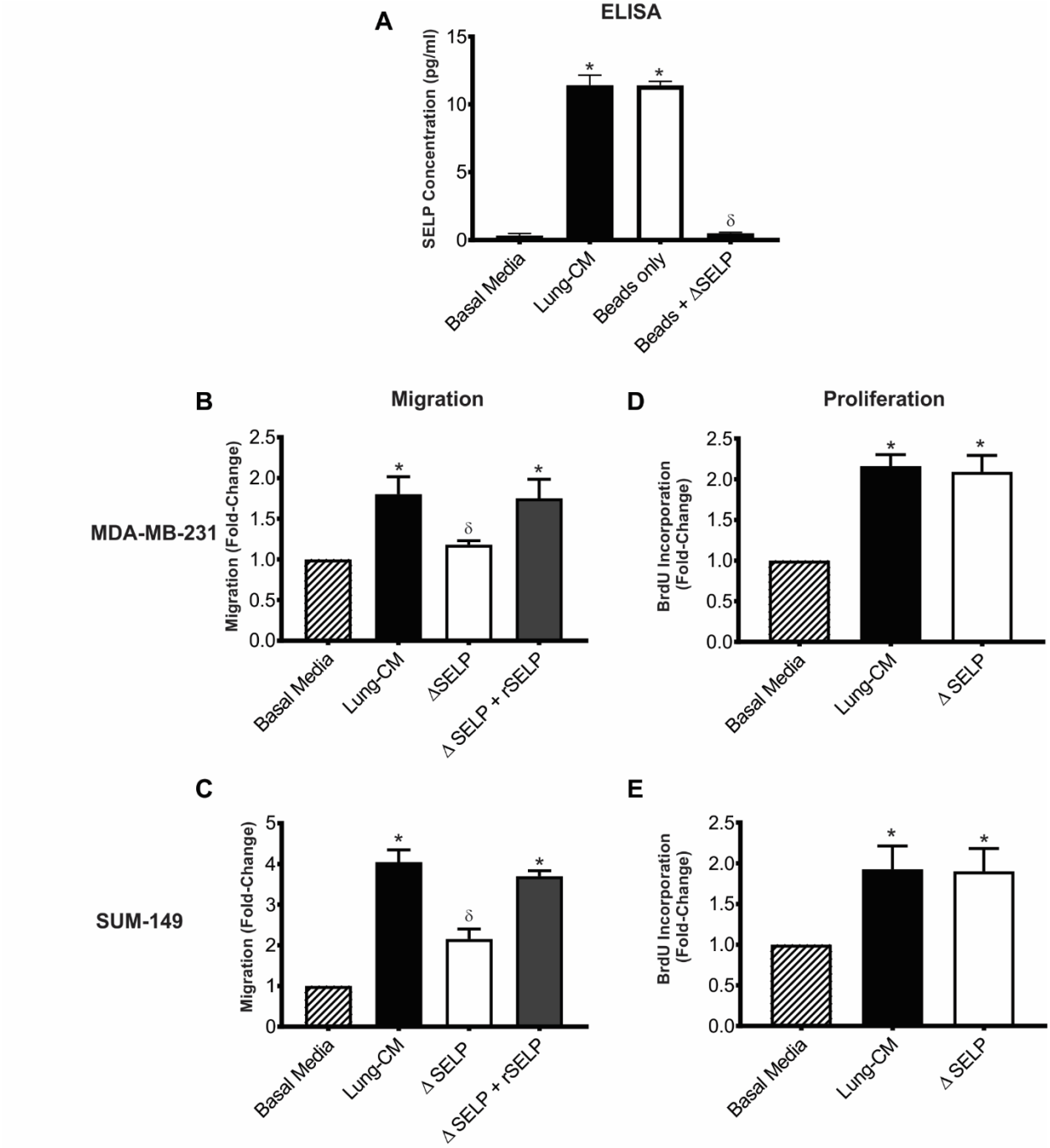

Figure 6: *Depletion of P-selectin (SELP) from lung conditioned media (CM) reduces breast cancer cell migration but not proliferation*. **(A)** Lung-CM was generated from healthy female mouse lungs and SELP immunodepleted. Resulting SELP protein levels were determined by ELISA. Data are presented as mean [SELP] ± SEM (n = 3). **(B,C)** MDA-MB-231 and SUM149 cell migration following exposure to basal media, native lung-CM, lung-CM depleted of SELP (ΔSELP), or ΔSELP rescued by re-addition of recombinant SELP. **(D,E)** MDA-MB-231 and SUM149 cell proliferation following exposure to basal media, native lung-CM, or lung-CM depleted of SELP (ΔSELP). Data are presented as mean fold-change in migration or BrdU incorporation relative to basal media ± SEM (n = 3). * = significantly different than basal media; δ = significantly different than native lung-CM ($p \leq 0.05$).

investigation of multiple pathways) and specific investigation of the ERM (ezrin, radixin, moesin) pathway that, when phosphorylated, have been shown to serve as a linker between CD44 and the cytoskeleton to facilitate migration. Our results demonstrate that ERM is phosphorylated in breast cancer cells following exposure to the lung microenvironment (***Figure 7A***).Furthermore, phospho-array analysis demonstrates that exposure of human breast cancer cells to the lung microenvironment results in phosphorylation of several other important downstream proteins including ERK1/2, MSK1/2, CREB, Lyn, and Src (***Figure 7B***). These array results have been validated by immunoblotting (*representative data for CREB shown in* ***Figure 7C***).

In conclusion, the major findings for this Task are that the CD44-interacting proteins OPN, FGF2, and selectins have complementary and important roles in mediating breast cancer metastatic behavior in response to the lung microenvironment, supporting the concept that that these lung-derived proteins are suitable therapeutic targets for further development.

Major Task 2: 3D *ex vivo* assessment of essential lung-derived factors.

The proposed work for Major Task 2 is complete and is described below. This work also supports ***Specific Aim 1.***

TASK 2.1: *Establish breeding colonies of knockout mice*

This task is 100% complete. OPN-/-, triple-selectin-/-, and FGF2-/- breeding colonies were successfully established and used for experiments (Task 2.3, described below). Although we had originally proposed to also look at single selectin knockouts (SELE-/-, SELP-/- , and SELL-/-), our *in vitro* data suggests that the 3 selectins may be compensatory for each other and therefore our focus has been on the pan-selectin knockout mice for the *ex vivo* studies. This approach is also well-aligned with the use of a pan-selectin inhibitor for the therapeutic studies (Tasks 4 and 5, described below).

TASK 2.2: *Transduce cell lines to stably express RFP*.

This task has been completed for all breast cancer models (see example in ***Figure 8E***).

TASK 2.3: *Assess the essentiality of each lung-derived factor for metastatic colonization/growth within the intact lung microenvironment in the 3D ex vivo PuMA.*

This task is 100% complete. Breast cancer cells have been subjected to the *ex vivo* PuMA using wildtype versus OPN-/-, triple-selectin-/- and FGF2-/- mice. The full set of these experiments has been completed in MDA-MB-231, SUM159, LRCP-BR17 and LRCP-BR21 breast cancer models, and the most significant results are presented in ***Figure 8***. Using breast cancer cells that are strongly metastatic to lung *in vivo* (MDA-MB-231, SUM159, LRCP-BR17), we observed that loss of OPN or E/L/P selectins significantly reduces (but doesn't completely eliminate) breast cancer progression to metastasis in the lung by Day 21 of the assay, whereas loss of FGF2 does not significantly alter breast cancer progression relative to wildtype (***Figure 8A,B,C,E***). Interestingly, in the breast cancer model that is non-metastatic to lung *in vivo* (LRCP-BR21), there is low level of metastatic growth/colonization in the PuMA overall, with no difference in wildtype versus any of the knockout mice (***Figure 8D***). Taken together, these results suggest that OPN and selectins (but not FGF2) are individually important for lung metastasis of breast cancer.

TASK 2.4: *Prepare and publish manuscript(s) from Specific Aim 1.*

This task is in progress but was delayed due to COVID19 (detailed in the Changes/Problems section). We anticipate submission of a primary data manuscript in November 2020.

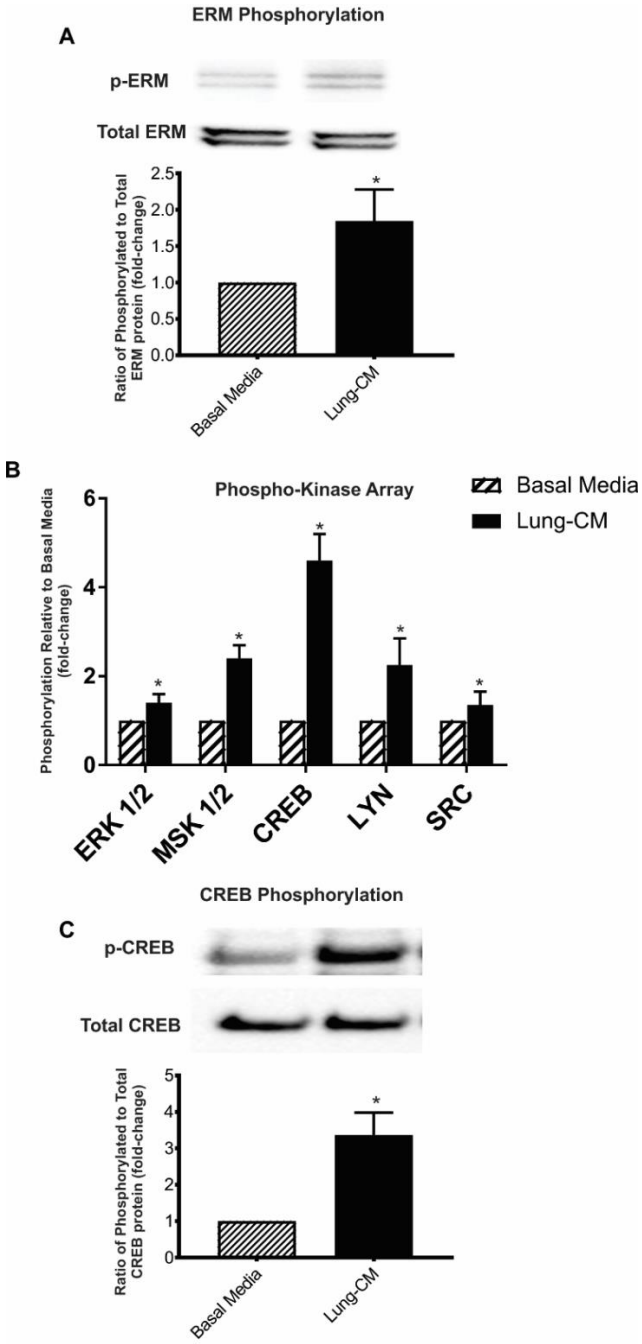

Figure 7: *Effect of lung-conditioned media (CM) on protein phosphorylation in human breast cancer cells*. MDA-MB-231 cells were cultured to 90% confluence and serum-starved for 24 h. Cells were then exposed for 15 min to basal media or native lung-CM and subjected to analysis by immunoblot or kinase array. Densitometry analysis was performed using Image Lab software (BioRad). Data is presented as fold-change in ratio of total:phosphorylated protein relative to basal media condition (n=3). **(A)** ERM phosphorylation as assessed by imunoblotting; **(B)** Broad investigation of protein phosphorylation using the Human Phospho-Kinase Array (R&D Systems); **(C)** Representative validation of CREB phosphorylation using immunoblot analysis. * = significantly different than basal media ($p \leq 0.05$). All other phosphorylation results were also validated by immunoblotting (*data not shown*).

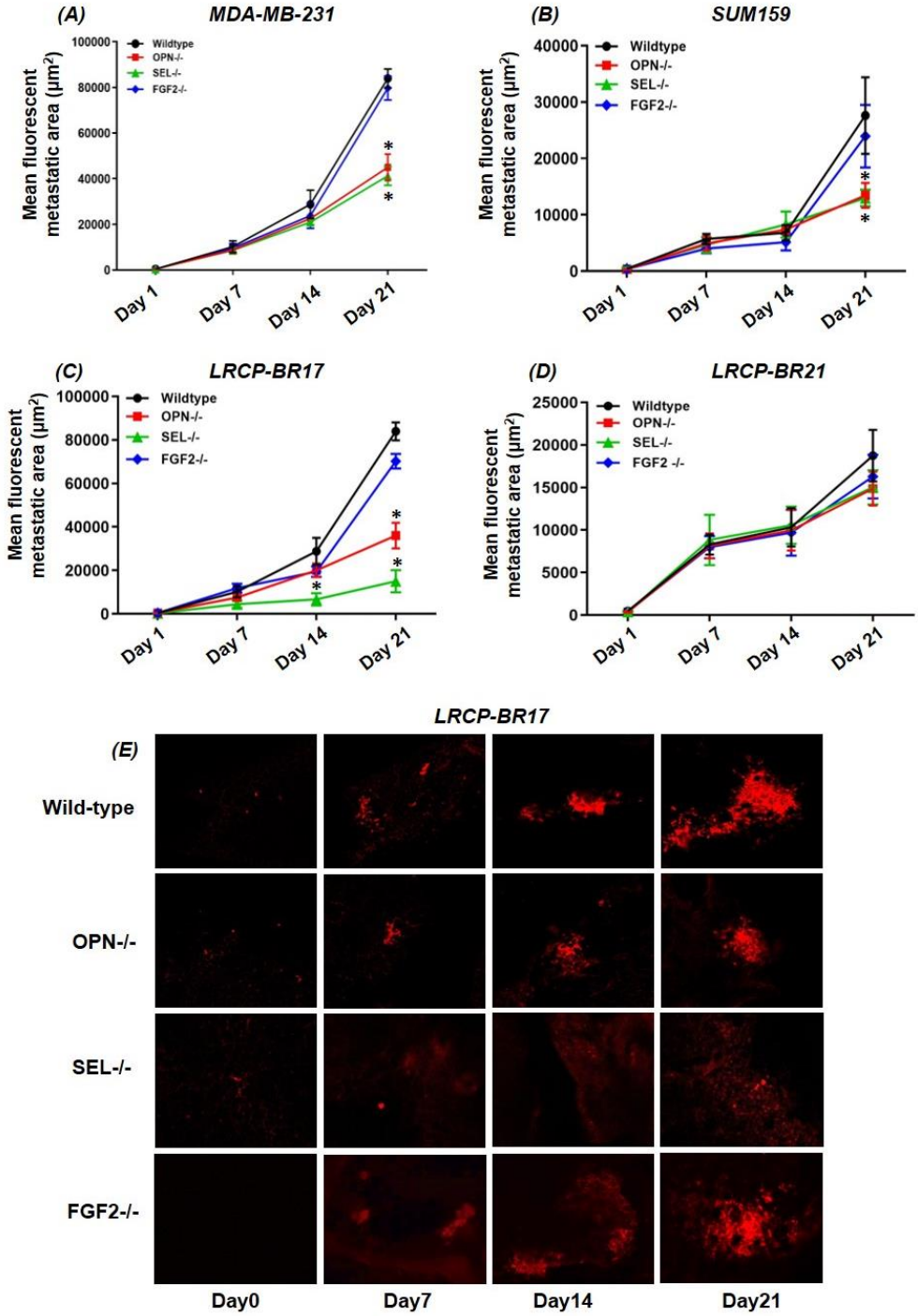

Figure 8: *Loss of OPN or E/L/P selectins but not FGF2 in the lung reduces breast cancer metastatic progression in the pulmonary metastasis assay (PuMA)*. To assess the essentiality of OPN, selectins, or FGF2 for metastatic progression in the *ex vivo* PuMA assay, red-fluorescent labeled MDA-MB-231 ***(A)***, SUM159 ***(B)***, LRCP-BR17 ***(C)*** and LRCP-BR21 ***(D)*** breast cancer cells were injected into wildtype (*black datasets*), OPN-/- (*red datasets*), triple-selectin-/- (*green datasets*), or FGF2-/- (*blue datasets*) mice, lungs were harvested after 15 minutes and subjected to the PuMA for 21 days (n=4 mice/dataset/cell line/timepoint). Data is presented as mean normalized fluorescent area (μm^2) ± SEM. * = significantly different than wildtype ($p \leq 0.05$). ***(E)*** Representative images for metastatic progression in the LRCP-BR17 model for each timepoint are shown.

In conclusion, the major accomplishments/findings for Task 2 to date include establishment of OPN-/-, triple selectin-/-, and FGF2-/- breeding colonies of knockout mice, which have been used to demonstrate that OPN and selectins (but not FGF2) are necessary for metastatic colonization of the lung, particularly for more aggressive breast cancer cell lines. This data provides a solid framework to move on to therapeutic application in Specific Aim 2.

Major Task 3: Formulation and production of an inhalable inhibitor

TASK 3.1: *Load inhibitors into polybutyl cyanoacrylate nanoparticles*; and
TASK 3.2: Assess and optimize NP drug loading efficiency/capacity.

These tasks are now 100% complete. Initial work was aimed at characterizing nanoparticles obtained from different monomers and synthesis route. A platform of different conditions that can be used to efficiently synthesize nanoparticles was developed. Assessment of different nanoparticles was made using the particle size (Z-average, nm), PdI (polydispersity index) and ease of synthesis as criteria. Parameters such as type and quantity of monomer, type and quantity of surfactants, stirring time, temperature, amount of solvent and purification method were varied for optimization.

Poly-butylcyanoacrylate nanoparticles: The poly-butylcyanoacrylate (PBCA) nanoparticles were prepared using n-butylcyanoacrylate (Loctite, Ireland) as monomer. The nanoparticles were prepared according to the following procedure: 100 µL of monomer was added to 1% dextran 70 (Sigma, Canada) solution in 10 mL of 0.01 M HCl under constant stirring at 600 rpm for 4 hours at room temperature. The particle size distribution was measured by dynamic light scattering using a photon correlation spectrometer (Zetasizer HAS 3000) from Malvern instruments. Both filtered (through a 0.1µm filter) and non-filtered samples were diluted 10 times in purified and degassed water and analyzed in triplicates. Good results were obtained using this method and the procedure was repeated at least in triplicate to guarantee reproducibility. PBCA nanoparticles were also prepared using a combination of 1% dextran 70 and 0.2% Pluronic F68 according to the aforementioned method. When measuring particle size, 1:10 and1:100 dilutions were used. Good results were obtained for this method as well, which are shown in ***Figure 9***.

Gelatin nanoparticles: Gelatin nanoparticles were prepared using a two-step desolvation process. Desolvation is the removal of the solvent component from the particle as a method of drying the sample in solution. In this case, the water was removed using acetone. Gelatin from two different manufacturers were tested. Three different batches from Gelita manufacturer were tested according to the following method: gelatin (1.25g) was dissolved in water (25ml) under constant heating (40ºC) and stirring at 550 rpm. After completely dissolved, acetone (25ml) was added into the gelatin in solution in order to precipitate the high molecular weight gelatin of the starting material. The supernatant was taken out and the precipitate was then resuspended in water (25 ml) under heating and stirring. The solution pH was changed to 2.5 using 0.1M HCl. Acetone (75ml) was added dropwise for the second step of the desolvation process under constant stirring at 550 rpm and heating at 40ºC. 100 ul of 8% glutaraldehyde was added into the mixture as a crosslinker and the mixture was stirred overnight. After completion of synthesis, the solvent was removed using a rotary vapor. The particles were resuspended in water and centrifuged at 80,000 rpm for 30 minutes. The pellet was suspended in purified and degassed water for characterization.

A

		Size (d.nm):	% Volume	Width (d.nm):
Z-Average (d.nm): 166.2	Peak 1:	175.0	100.0	60.98
PdI: 0.076	Peak 2:	0.000	0.0	0.000
Intercept: 0.948	Peak 3:	0.000	0.0	0.000
Result quality : Good				

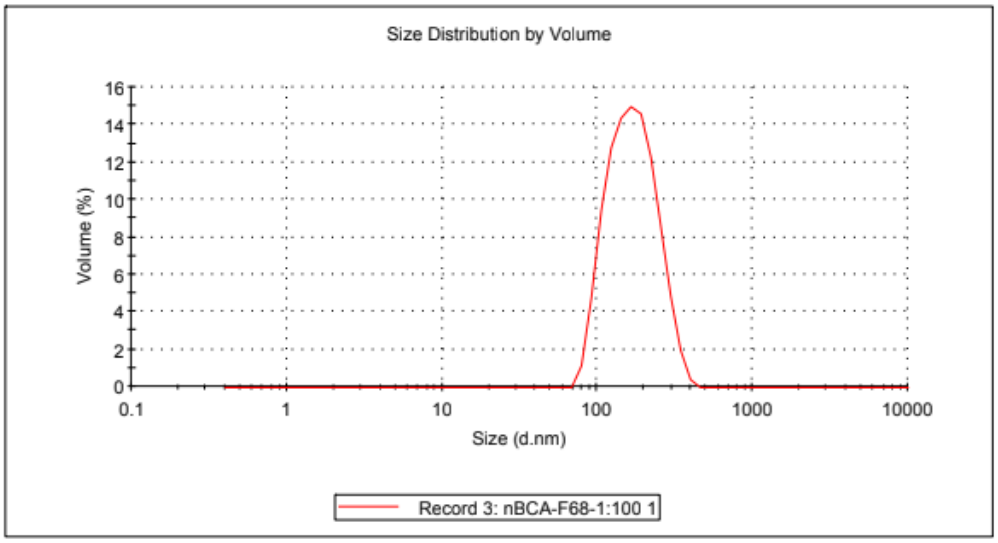

B

		Size (d.nm):	% Volume	Width (d.nm):
Z-Average (d.nm): 169.3	Peak 1:	177.7	100.0	56.59
PdI: 0.058	Peak 2:	0.000	0.0	0.000
Intercept: 0.955	Peak 3:	0.000	0.0	0.000
Result quality : Good				

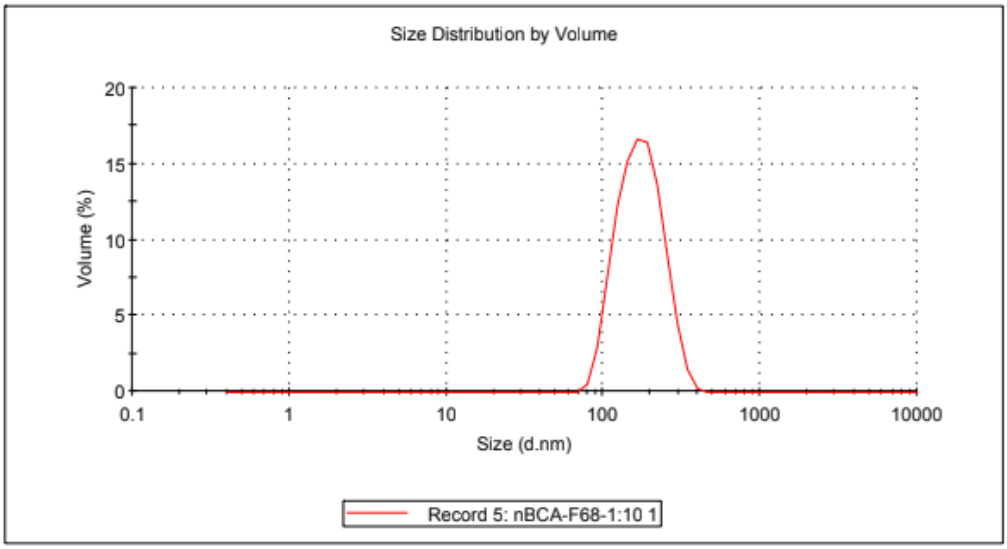

Figure 9. *Particle size (diameter, nm) and PdI of PBCA nanoparticle prepared with dextran 70 and Pluronic F68*. **(A)** Dilution factor of 100. **(B)** Dilution factor of 10

As shown in ***Figure 10A***, for the first batch, a sharp peak was obtained, nevertheless the particles were too big. For the second batch (***Figure 10B***), although the particle size was big, a good PdI was obtained as well as a sharp peak. For the third batch, no precipitation occurred in the first desolvation step. Gelatin nanoparticles using gelatin Type B from bovine skin (Sigma-Aldrich) were prepared using the aforementioned method. The method showed poor quality results and low yield. The method was then optimized varying the water/acetone ration and amounts, different amount of starting material, temperature, concentration of cross-linker, probe sonication of sample, ultrafitration vs. centrifugation vs. filtration and different gelatin starting material. The best result obtained (***Figure 11***) was using gelatin type B from bovine skin 225 bloom (Sigma-Aldrich), using 1g of starting material, water/acetone ratio of 1:1 (20 ml); the first precipitate was dissolved in water under vigorous stirring at 10,000 rpm and 50ºC. Acetone (20ml) was added dropwise and stirred for one hour. After acetone evaporation, samples were centrifuged at 10,000g for 30 minutes and the pellet was resuspended in water followed by filtration through a 0.22um syringe filter.

Nanoparticle properties after drug loading: PBCA nanoparticle was selected to continue with the drug loading and antibody-coating experiments due to ease of synthesis, high yield, good quality and reproducibility. Doxorubicin was used as the model drug to optimize the drug loading. The drug was added in the mixture after 30 minutes of stirring. Particles were characterized after drug loading. Results showed satisfactory particle size and PdI, 140 nm (±10.56) and 0.159 (±0.027), respectively

Antibody coating: PBCA nanoparticles prepared with dextran 70 and Pluronic F68 were used for the antibody coating due to the presence of aldehyde groups on its surface that the antibody can be adsorbed onto. MBU-monoclonal antibody was used as a model for this purpose. The nanoparticles were incubated with 100ug/ml of the antibody in different settings: in a beaker shaking at room temperature or at 4ºC or in an Eppendorf rotating at room temperature or at 4ºC (3). The samples were then centrifuged at either 12.5 rpm for 20 minutes or 24psi for 30 minutes. The supernatant was separated and used for ELISA testing. It was assumed that low supernatant antibody concentration was due to adsorption onto the particles.

ELISA procedure: Antigen solution was prepared (myclobutanil and myclobutanil-BSA conjugate) (10 ug/mL) in coating buffer (0.01M Carbonate/bicarbonate, pH 9.4-9.6) and 100 uL was added to each well onto the 96 well assay plate, including buffer control and negative control. The plate was covered and incubated at 2-8 °C overnight. The solution was aspirated and adherent drops were removed by tapping the inverted plate on a piece of paper towel. 300 ul of wash buffer (PBS containing 0.05% Tween-20) was added to each well and aspirated, this procedure was repeated three times. Blocking buffer (300 ul - PBS containing 1% BSA) was added to each well and the plate was kept at room temperature for 1 h. The plate was then washed three times. The supernatant of the samples previously prepared with antibody and PBCA nanoparticles were diluted with blocking buffer and pipetted to the required wells. The plate was incubated at 37°C for one hour. The plate was washed and secondary antibody (diluted HRP-conjugated goat anti- mouse IgG antibody) was added to all the sample wells except substrate control wells and the plate was incubated at 37°C for 30 minutes. After washing plate, the substrate solution was added to each well followed by incubation at 37°C for 15/30 minutes. Absorbance was measured at 405 nm on an automatic ELISA plate reader. ***Table 1*** shows the absorbance results.

A

			Size (d.nm):	% Volume	Width (d.nm):
Z-Average (d.nm):	2313	Peak 1:	1165	100.0	167.5
PdI:	1.000	Peak 2:	0.000	0.0	0.000
Intercept:	0.968	Peak 3:	0.000	0.0	0.000
Result quality :	Refer to quality report				

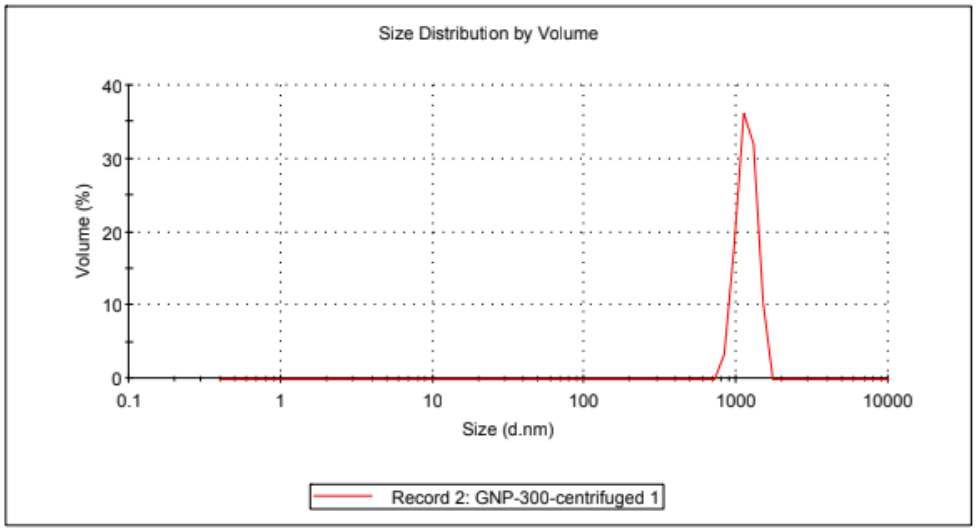

B

			Size (d.nm):	% Volume	Width (d.nm):
Z-Average (d.nm):	816.2	Peak 1:	888.7	100.0	156.9
PdI:	0.077	Peak 2:	0.000	0.0	0.000
Intercept:	0.945	Peak 3:	0.000	0.0	0.000
Result quality :	Refer to quality report				

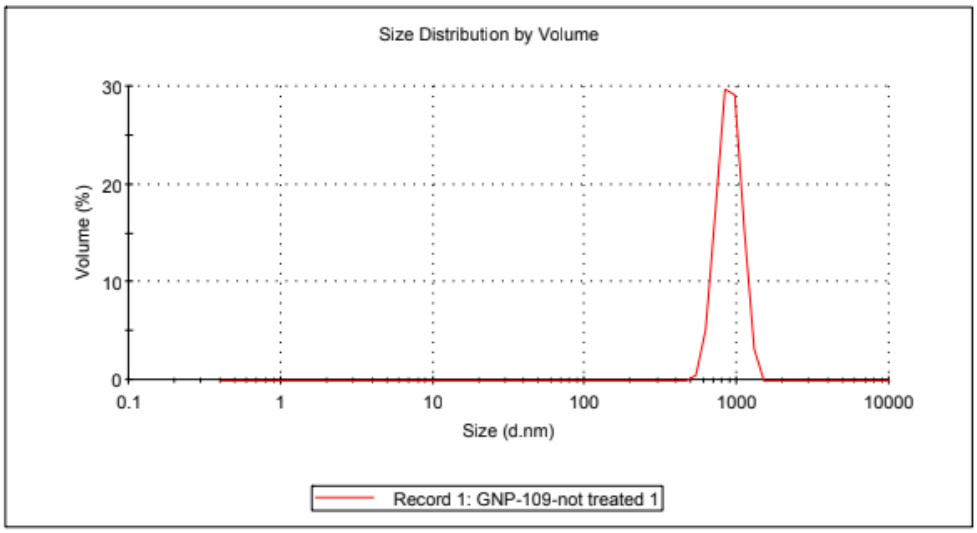

Figure 10. *Particle size (diameter, nm) and PdI of gelatin nanoparticle using different batches from Gelita manufacturer*.

			Size (d.nm):	% Volume	Width (d.nm):
Z-Average (d.nm):	224.4	Peak 1:	266.9	100.0	99.48
PdI:	0.126	Peak 2:	0.000	0.0	0.000
Intercept:	0.889	Peak 3:	0.000	0.0	0.000
Result quality :	Good				

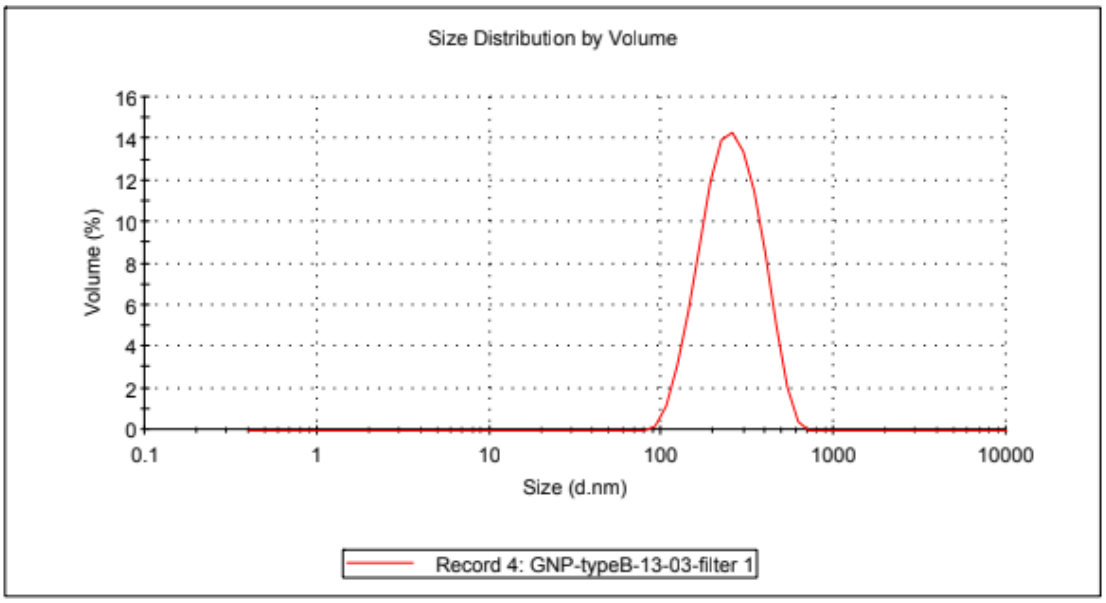

Figure 11. Particle size (diameter, nm) and PdI of gelatin nanoparticle using gelatin type B from bovine skin.

Table 1

15 minutes incubation for color development

	1	2	3	4	5
A		0.1685	0.2108	0.1429	0.1236
B	Control	0.1151	0.0912	0.0997	0.0973
C	Standard	0.2039	**0.2207**	0.3782	**0.4015**
D	Standard	0.1904	**0.3844**	0.3786	**0.3448**
E		0.1402	0.1231	**0.1412**	**0.4246**
F		0.1102	0.1182	**0.0777**	**0.3944**
G		0.1422	0.1097	0.111	0.1066
H		0.0901	0.1029	0.0939	0.0819

30 minutes incubation for color development

	1	2	3	4	5
A		0.2514	0.2888	0.212	0.1818
B	Control	0.1708	0.1341	0.1431	0.1245
C	Standard	0.2964	**0.4368**	0.5243	**0.547**
D	Standard	0.324	**0.7246**	0.5549	**0.555**
E		0.2306	0.1706	**0.1772**	**0.6042**
F		0.1641	0.1739	**0.1278**	**0.58**
G		0.2145	0.1615	0.1424	0.1469
H		0.127	0.148	0.1385	0.1208

Color code and legends:

1	2	3	4	5	
Control	CB+PBS+2AB+S		x	x	
Control	Ag+PBS+2AB+S				
Standard: 1AB concentrations	10ug/ml	**25ug/ml**	50ug/ml	**100ug/ml**	
	10ug/ml	**25ug/ml**	50ug/ml	**100ug/ml**	
	RTs C		**RTs A**	**100**	Ag+1AB+2AB+S
	Ice C		**Ice A**	**100**	
	RTr C		RTr A	x	
	Ice'C		x	x	

TASK 3.3: *Incorporate optimized drug-loaded NPs into inhalable effervescent carrier particles; &*
TASK 3.4: *Quality assurance assessment of inhalable drugs*

Following this optimization and the results obtained to date for Task 2, we moved forward with optimizing the use of the pan-selectin antagonist bimosiamose as an inhalable drug for lung metastasis. This choice of inhibitor was supported by both the results of Specific Aim 1, as well as additional *in vitro* studies demonstrating that bimosiamose (1 mM) effectively inhibits breast cancer proliferation and migration in response to lung-conditioned media (***Figure 12***).

The selected pan-selectin antagonist bimosiamose is an organic compound that belongs to the phenolic glycoside class. Its physicochemical properties are displayed in ***Table 2***. The high lipophilicity and low water solubility of bimosiamose make it an ideal candidate for the use of nanocrystals as a drug delivery system. The reduction of the particle size into the nanometer scale is a promising approach for hydrophobic drugs in order to increase surface area which, in turn, increases the dissolution rate and solubility of poorly water-soluble compounds like bimosiamose. This is specially desired for the inhalable route of administration, since the drug has to dissolve in the low volume of pulmonary fluids.

The nanocrystal production was done using the wet bead milling process. During the stirring (high shear forces), the drug particles collide with the zirconia beads in the milling chamber, and with other drug particles, causing the drug crystals to be fractured into nanosized particles. Shear forces in the liquid phase are stronger compared to dry milling. In order to verify the best conditions and the system's suitability to reduce the particle size of bimosiamose, a compound with similar physicochemical properties was used as model (***Table 2***). Hence, this study was aimed to characterize nanocrystals obtained by wet milling process under a range of conditions with the goal to further optimize the process using the model drug erythromycin ethylsuccinate.

At an early research stage, as well as at an early stage in drug development, only small quantities of the active compound are available. Hence, using a particle size reduction method which requires only low amounts is essential. The miniaturized wet bead milling method is a valuable approach in this setting. The system is composed of an aqueous dispersion media (in which the drug has low solubility) containing stabilizers (surfactants, polymers, or both), milling pearls (zirconia beads), two magnetic stirring bars and the drug. The system is agitated by a magnetic stirring plate at a very high speed, which is the reason why stabilizers are necessary.

Preparation of nanosuspension by miniaturized wet bead milling method: Erythromycin ethylsuccinate (EE) nanosuspension was prepared by wet bead milling at a reduced scale. The system contained 3% (w/w) EE, 10 to 20% of zirconia beads (0.1 mm and density 3.7 g/cm3) and a 3% (w/w) Povacoat® (a novel PVA copolymer) aqueous solution of pH 5.7 for a total weight of 1g. The milling chamber consisted of a 2 mL glass vial containing two magnetic stir bars, polygon-shaped (8x2mm). The system was stirred at 800 rpm for up to 8 days at room temperature. Samples of 10µL were collected each day.

Particle size distribution: The particle size distribution (PSD) as well as the poly-dispersity index (PdI) were measured by dynamic light scattering using a photon correlation spectrometer (Zetasizer HAS 3000) from Malvern instruments. Samples were diluted to a suitable concentration, indicated by the best attenuation coefficient. Both purified degassed water and saturated EE solution were used to measure the PSD to identify if the particles would partially dissolve when prepared for the measurements with pure water, giving a false smaller particle size.

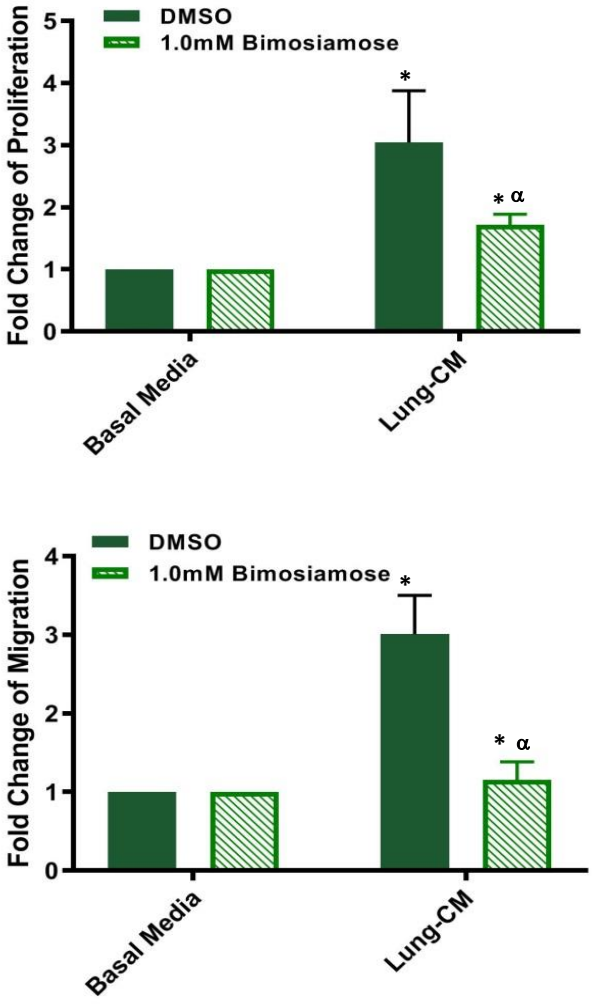

Figure 12: *The pan-selectin antagonist bimosiamose reduces breast cancer cell proliferation and migration in the presence of lung-conditioned media*. MDA-MB-231 cell proliferation (*top panel*) and migration (*bottom panel*) following exposure to basal media or native lung-CM and treatment with DMSO vehicle or bimosiamose (1 mM). Data are presented as mean fold-change in transwell migration or BrdU incorporation relative to basal media ± SEM (n = 3). * = significantly different than basal media; α = significantly different than lung-CM ($p \leq 0.05$).

Table2. Physicochemical properties of bimosiamose and erythromycin ethylsuccinate

	BIMOSIAMOSE	ERYTHROMYCIN ETHYLSUCCINATE
CHEMICAL STRUCTURE	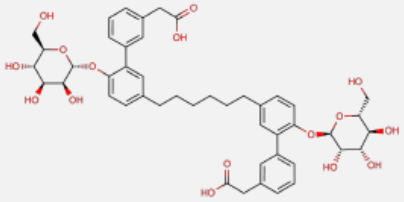	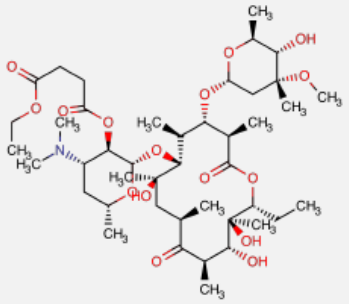
Molecular weight (g/mol)	862.922	862.064
Log P	3.71	3.37
Log D (@ pH 5.7)	0.603	0.652
Log S (@ pH 5.7)	-3.8	0.133

Figure 13 shows the monitoring of the PSD of a nanosuspension system with 3% EE (w/w), 17% beads (w/w) and 3% stabilizer. Different populations can be identified during the first day of stirring, which is also reflected on the high PdI. The stirring and the PSD monitoring continued for 7 days. Not much difference was seen between days 2 and 3 (***Figure 14***). After 3 days stirring the PdI was within an acceptable range (only 1 population of nanocrystals) and the average particle size was 740 nm. After 7 days stirring a PSD of 458nm was obtained with an even lower PdI (***Figure 15***). Using water to dilute the samples did not give accurate measurements, as shown in ***Figure 16***.

FINAL OPTIMIZATION OF INHALABLE BIMOSIAMOSE

Particle size reduction into the nanometer scale is a promising approach to increase the dissolution of hydrophobic drugs such as bimosiamose. The drug particles are constituted as matrix-free nanocrystals and are stabilized by surfactants, polymers, or a mixture of both. This system (stabilizer and crystals) is called a nanosuspension.

Different approaches can be taken to produce nanocrystals, such as top-down methods. Wet media milling is one example of such, in which large particles are broken into small sized particles using mechanical grinding. The miniaturized wet-bead milling system consists of a milling glass chamber filled with zirconia beads, the drug substance, a dispersion media (stabilizer in aqueous solution), and magnetic stirring bars. This system is agitated by a magnetic stirrer plate at high speed. The advantages of this is that it is a simple and low-cost method which is performed in small volumes, providing advantages in early drug development.

The stabilizing agents (surfactants and polymers) play an important role in particle size reduction and stability of nanosuspensions. In this study we screened different stabilizers (namely: Hydroxypropyl cellulose (HPC), Polyvinyl alcohol (PVA), Polyvinylpyrrolidone (PVP), Poloxamer 188 and Povacoat) to be used in the wet milling process, all of which are GRAS and have been reported to be used in inhalable therapies. Since nanocrystals, due to their small size, tend to get stuck in the upper airways, they were incorporated into microcarriers. This will enable the powder to reach the deep lung.

Preparation of nanosuspension by miniaturized wet bead milling method: A bimosiamose nanosuspension was prepared by wet bead milling at a reduced scale. The system contained bimosiamose (10 mg), zirconia beads (0.5 g) and a stabilizer aqueous solution (0.5 mL) (HPC, PVA, PVP, Poloxamer 188 or Povacoat). The milling chamber consisted of a 2 mL glass vial containing two magnetic stir bars, polygon-shaped (8x2 mm). The system was stirred at 800 rpm at room temperature up to 48hrs depending on the stabilizer used. For HPC, PVA, PVP and Povacoat, the proportion between stabilizer and drug was 4:1 and for Poloxamer 3:1.

Particle size distribution and stabilizer screening: The particle size distribution (PSD) as well as the polydispersity index (PdI) were measured by dynamic light scattering using a photon correlation spectrometer (Zetasizer HAS 3000) from Malvern instruments. Samples were diluted to a suitable concentration, indicated by the best attenuation coefficient. The PSD results are indicated as size distribution by volume.

Results

			Size (d.nm):	% Volume	Width (d.nm):
Z-Average (d.nm):	1364	Peak 1:	837.9	80.5	134.6
PdI:	0.868	Peak 2:	87.60	19.5	13.80
Intercept:	0.946	Peak 3:	0.000	0.0	0.000
Result quality :	Refer to quality report				

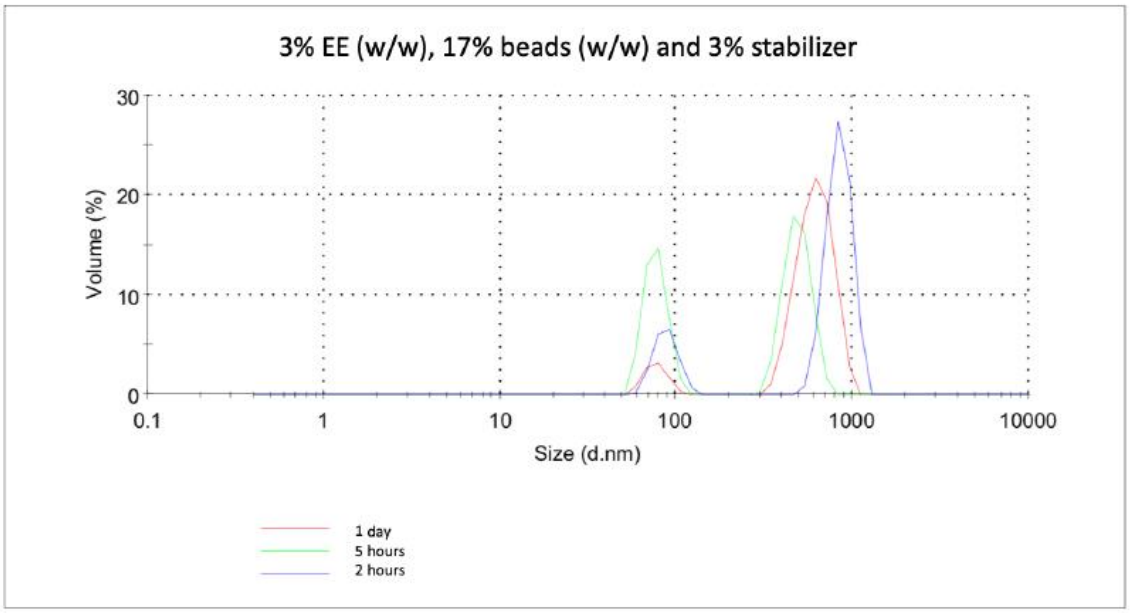

Figure 13. Particle size distribution (diameter, nm) and PdI of EE nanocrystals prepared with 3% EE (w/w), 17% beads (w/w) and 3% stabilizer at 2 hours, 5 hours and 24 hours.

Results

			Size (d.nm):	% Volume	Width (d.nm):
Z-Average (d.nm):	740.4	Peak 1:	1164	98.8	355.7
PdI:	0.263	Peak 2:	172.4	1.2	46.34
Intercept:	0.939	Peak 3:	0.000	0.0	0.000
Result quality :	Good				

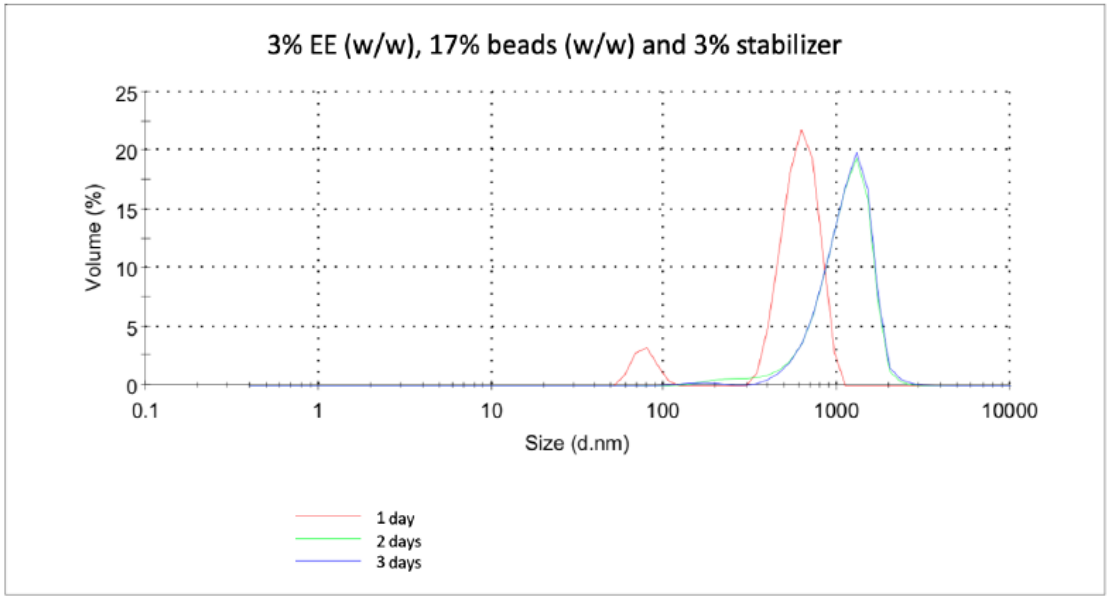

Figure 14. Particle size distribution (diameter, nm) and PdI of EE nanocrystals prepared with 3% EE (w/w), 17% beads (w/w) and 3% stabilizer after 3 days stirring.

Results

		Size (d.nm):	% Volume	Width (d.nm):
Z-Average (d.nm): 458.8	Peak 1:	738.3	100.0	304.9
PdI: 0.195	Peak 2:	0.000	0.0	0.000
Intercept: 0.953	Peak 3:	0.000	0.0	0.000
Result quality : Good				

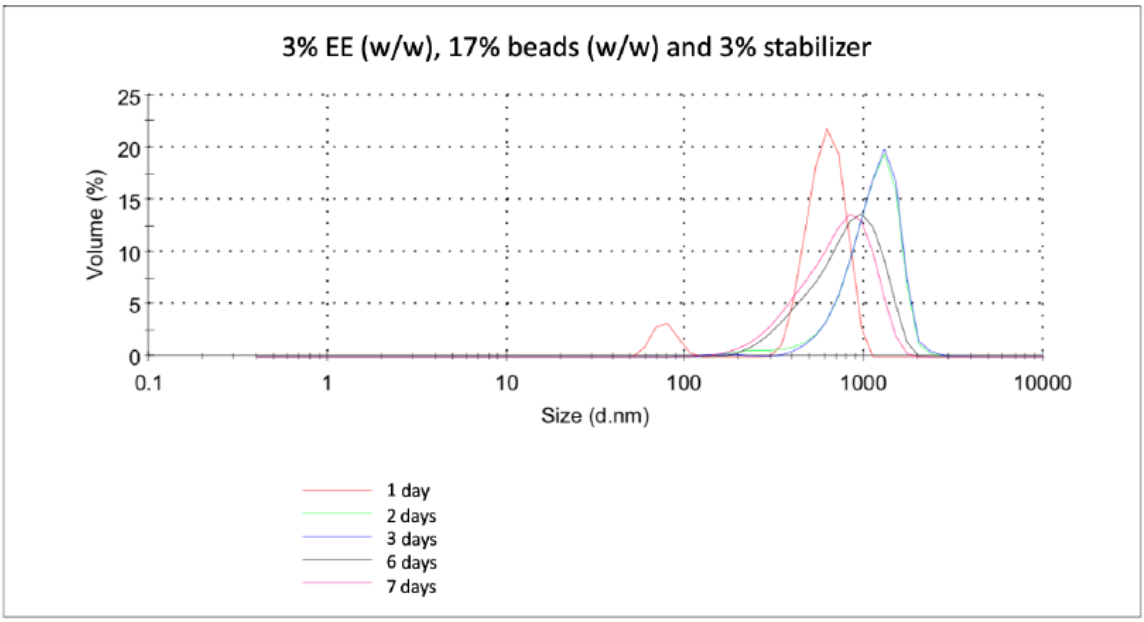

Figure 15. Particle size distribution (diameter, nm) and PdI of EE nanocrystals prepared with 3% EE (w/w), 17% beads (w/w) and 3% stabilizer after 7 days stirring.

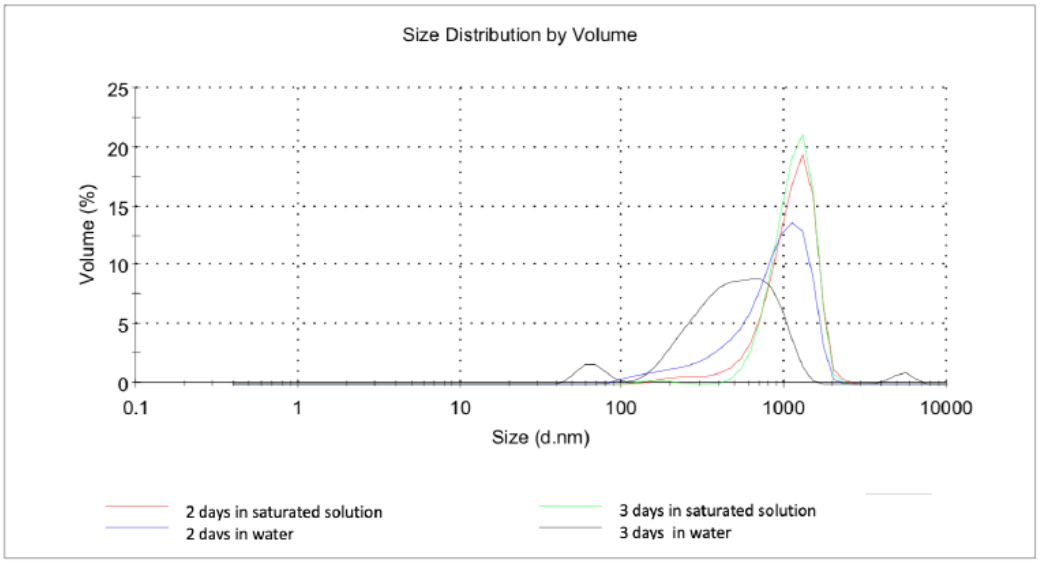

Figure 16. PSD (diameter, nm) of EE nanocrystals in water and saturated solution.

Povacoat: For Povacoat, the samples were collected for analysis at 1h, 24hrs, 36hrs and 48 hrs. ***Table 3*** shows the Z-average for the PSD of the nanosuspension system (done in triplicate) at the different collection time points. Different populations could be identified during the first hour of stirring. Povacoat was initially developed as a film-coating agent, wet granulation binder and solid dispersion matrix, but recent studies revealed its use as a stabilizer to prevent aggregation of nanocrystals. Because it formed a dispersion when added to water, we investigated the particle size of Povacoat alone in water (***Figure 17***). Notably, Povacoat dispersion is also in a nano scale. Hence, in order to minimize confounding factors in the PSD measurements, other stabilizers were screened: HPC, PVA, PVP and Poloxamer 188. These were completely dissolved in water, resulting in a stabilizer solution instead of a suspension.

Povacoat, HPC, PVA, PVP and Poloxamer 188: Based on the results using Povacoat, the stirring time was set to 24 hours. ***Table 4*** shows the Z-average for the PSD of the nanosuspension system for the different stabilizers, including a second trial using Povacoat (for comparison purposes and repeatability assessment).Based on the Z-average and PdI results, and considering its wide use in inhalable systems, Poloxamer 188 was the stabilizer of choice.

Poloxamer 188: In order to obtain particles with bigger particle size the stirring time was reduced to 2hrs (***Table 5***). To assess the repeatability of the selected system, other batches were prepared using the 2hrs stirring time and the result was consistent (Z-avg: 117.8nm; PdI: 0.120).

Microcarrier preparation: The optimized nanosuspension formulation was spray-freeze dried using a carrier agent. The agents investigated were lactose and mannitol. Lactose was not a feasible agent; hence mannitol was used in this study. The following parameters were used for the spraying process: atomized air pressure: 1bar; spray rate: 0.49 ml/min; liquid nitrogen volume kept constant at 700 ml, spray nozzle positioned 10cm above the liquid nitrogen level. Once sprayed, the samples were lyophilized overnight. The mass median aerodynamic diameter (MMAD) of the powder was measured using the Penn-Century dispersing device coupled to an aerosol diluter and an aerodynamic particle sizer (APS). A small scale powder disperser (SSPD) coupled to the APS was also test to compare the MMAD results using different dispersing setups (***Figure 18***). The MMAD determines the deposition location of particles within the lungs. A size between 2-5 μm is usually desired to reach the deep lung. However, the obtained value is borderline and may potentially still reach the alveolar system. As we move into animal testing in Major Tasks 4 and 5, we are in the process of prepare a second batch of inhalable drug using a lower spraying rate to increase MMAD value

Major Tasks 4 and 5*: In vivo* assessment of anti-metastatic efficacy of inhalable drugs using preventative and therapeutic approaches

These two tasks have been delayed due to COVID19 (detailed in the Changes/Problems section). However, Major Task 4 has just been initiated in August 2020 with initial *in vivo* pilot experiments (in progress, no data to report yet). We anticipate that Major Tasks 4 and 5 will be completed by the end of the grant term in August 2021.

Table 3. Particle size distribution (diameter, nm) and PdI of bimosiamose nanocrystals prepared with Povacoat.

Time	Z-avg (nm)	PdI	Number of peaks
1 hour	127.7	0.234	2 (150.3 and 4779 nm)
24 hours	130.9	0.108	1
36 hours	120.5	0.104	1
48 hours	108.1	0.106	1

Table 4. Particle size distribution (diameter, nm) and PdI of bimosiamose nanocrystals prepared with different stabilizers.

Stabilizer	Z-avg (nm)	PdI
Povacoat	91.43	0.110
HPC	123.9	0.159
Poloxamer 188	83.72	0.102
PVP	83.76	0.102

Table 5. PSD (diameter, nm) and PdI of bimosiamose nanocrystals prepared with Poloxamer 188.

Time	Z-avg (nm)	PdI
2hrs	115.70	0.140
4.5hrs	99.61	0.124
5.5hrs	92.00	0.116

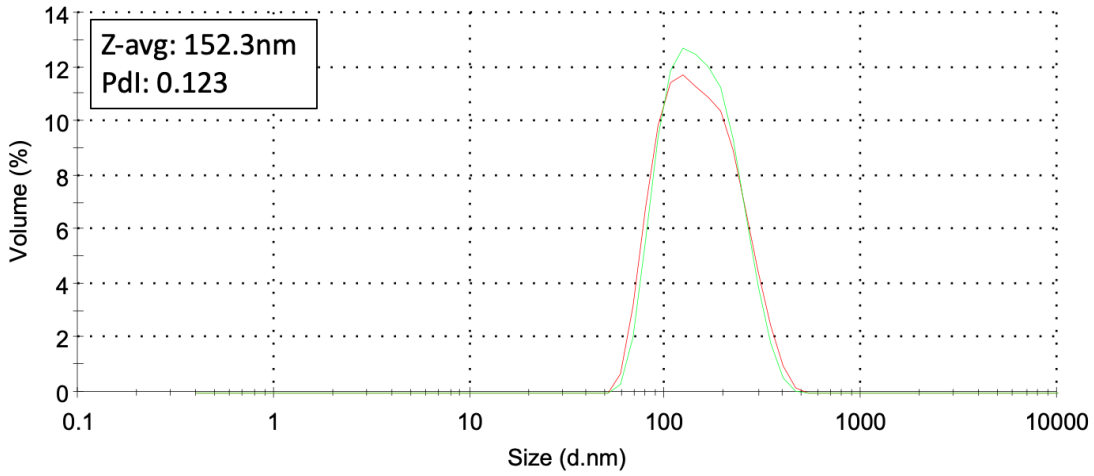

Figure 17. Particle size distribution (diameter, nm) and PdI of Povacoat alone in water.

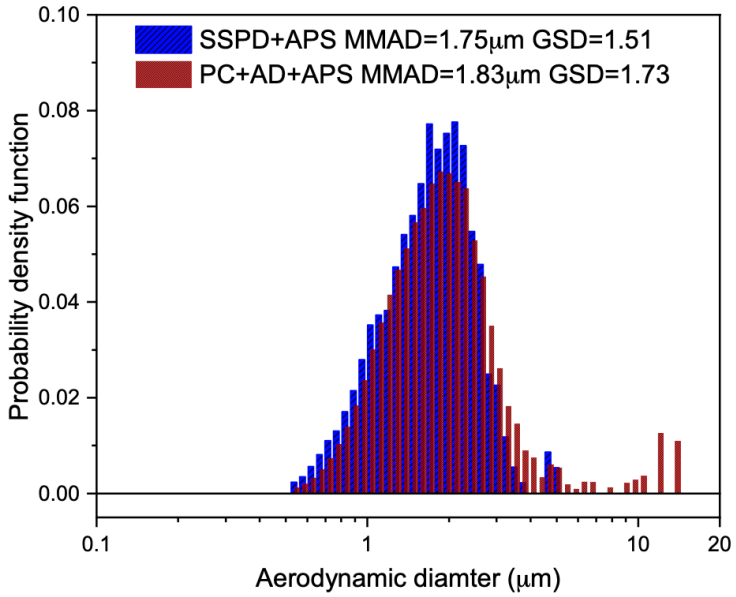

Figure 2. MMAD of mannitol carrier particles loaded with bimosiamose nanocrystals

➢ What opportunities for training and professional development has the project provided?

Training Opportunities

Dr. Ying Xia, Research Associate:

As part of this project, Dr. Xia provided one-on-one mentorship to 1 research undergraduate student, Gabriella Schoettle, 1 PhD student, Braeden Medeiros, and a new postdoctoral fellow, Dr. Vasu Bhat, all of whom contributed to the major research activities of the project. Dr. Xia assisted these trainees in attaining greater proficiency in experimental techniques including cell culture and data analysis.

Dr. Vijay Somayaji, Research Manager:

As part of this project, Dr. Somayaji provided one-on-one mentorship to 1 graduate student, Daniela Amaral-Silva, who contributed to the major research activities of the project as described above. Dr. Somayaji assisted Daniela in attaining greater proficiency in pharmaceutical and drug formulation techniques.

Professional Development Opportunities

Dr. Alison Allan, PD/PI:

To further her knowledge and skills in the area of breast cancer metastasis, Dr. Allan participated in the Canadian Cancer Research Conference which was held in Ottawa, Canada in November 2019.

➢ How were the results disseminated to communities of interest?

A. Scientific Publications

Bhat V, Lefebvre C, Goodale D, Rodriguez-Torres M, **Allan AL**. Isolation and functional assessment of human breast cancer stem cells from cell and tissue samples. 2020 *JoVE,* In press (*accepted manuscript appended*).

B. Scientific Presentations

David Goodale, Technician:

Goodale, D., Xia, Y., Postenka, C., and **Allan, A.L.** Knockout of lung-derived osteopontin or selectins reduces metastatic colonization in an *ex vivo* model of breast cancer lung metastasis. 2019 Canadian Cancer Research Conference, November 2019, Ottawa Canada.

Daniela Amaral-Silva, PhD student

November 2019, San Antonio TX - American Association of Pharmaceutical Sciences Annual Meeting - AAPS PHARMSCI 360. Daniela attended the conference and presented two posters titled “Delayed release drug products behave differently in physiological bicarbonate buffer” and “In Vitro Biphasic Dissolution Test: A Study of Excipient and Manufacturing Variables”

Dr. Alison Allan, PD/PI:

Allan, A.L. Role of the lung microenvironment in mediating breast cancer metastasis: a balance between the “seed” and the “soil”. Department of Anatomy & Cell Biology Seminar Series, Schulich School of Medicine & Dentistry, Western University, London ON, January 2020.

C. Community Outreach Activities

Dr. Alison Allan, PD/PI:

1. *Media Story*, **Allan A.L.** and Hill, D. Layoffs, lost funding and how COVID-19 may permanently hurt London's medical-research sector. April 6, 2020, London Free Press.

2. *Research Ambassador*, **Allan A.L.** Why is research important? Media interview on the Weather Network to kick off Breast Cancer Awareness Month. October 01, 2019 [TV media]

- **What do you plan to do during the next reporting period to accomplish the goals?**

Now that the drug formulation studies are completed and we have moved into the final pre-clinical *in vivo* studies, there is a high level of integration between the Allan and Loebenberg laboratories to complete the planned studies for the final Major Tasks of the project. We expect that this will contribute greatly to accomplishing our goals as laid out in the SOW.

4. IMPACT:

- **What was the impact on the development of the principal discipline(s) of the project?**

Nothing to Report.

- **What was the impact on other disciplines?**

Nothing to Report.

- **What was the impact on technology transfer?**

Nothing to Report.

- **What was the impact on society beyond science and technology?**

Nothing to Report.

5. CHANGES/PROBLEMS:

- **Changes in approach and reasons for change**

Nothing to Report.

- **Actual or anticipated problems or delays and actions or plans to resolve them**

Major Task 1:

No delays experienced.

Major Task 2:

Establishment of all planned breeding colonies of knockout mice was a bit slower than expected due to problems with some breeding pairs, however we worked closely with our animal facility veterinarian and these problems were resolved. We also had a delay in finishing the final set of *ex vivo* experiments with FGF2-/- mice due to the COVID19 research shut down between March 17, 2020 and July 02, 2020, which in turn delayed a planned primary publication. We completed these experiments as soon as research activities were allowed to resume, and expect to submit the publication by November 2020.

Major Task 3:

There was a slight delay at the start of the project in recruiting a PhD student with the appropriate expertise to work on the drug formulation aspect of the project under Dr. Loebenberg. Daniela Amaral-Silva was successfully recruited and has been actively working on the project since January 2018. There was also a delay/problem in obtaining stocks of the pan-selectin inhibitor Rivipansel from Pfizer. Pfizer is experiencing production issues and has to prioritize drug supplies for use in an ongoing human clinical trial. They are unsure when this is going to be resolved, so in May 2018 we decided to go ahead with an alternative pan-selectin inhibitor, Bimosiamose (MedKoo Biosciences). This inhibitor required custom synthesis and QA/QC, which was a 3-4 month process. We received the drug in November 2018, at which point we began the initial studies presented in this report.

Major Tasks 4 & 5:

We were on track to begin the in vivo experiments in March 2020, but were delayed by the COVID19 research shut down between March 17, 2020 and July 02, 2020. Large animal experiments were not permitted in the initial phases of re-opening, however in late August 2020 we received permission to move ahead with the first animal experiments for Major Task 4, with Major Task 5 to follow in early 2021.

- **Changes that had a significant impact on expenditures**

The delay in recruiting Daniela Amaral-Silva had an impact on the salary expenditures in Year 1 (only 6.5 person months worked instead of 12). The upgrades to the spray dryer equipment were purchased and delivered to Dr. Loebenberg's lab later than expected, with the final installation of spray dryer occurring in the late Fall of 2018. The equipment portion of the budget was therefore also not invoiced/recovered until installation was completed, in Year 2 of the project.

The COVID19 research shut down between March 17, 2020 and July 02, 2020 resulted in a reduction in expenditures for consumables and animals, since experimental work was put on hold. However, salaries continued to be paid as per the mandates of our institutions and employees were able to carry out many research activities from home (i.e. data analysis, writing, experimental design and planning). We requested and were granted a 12-month no-cost extension (to August 14, 2021) to complete Major Tasks 4 & 5. To complete this work, the remaining funds will support consumables, animals, and salaries.

- **Significant changes in use or care of human subjects, vertebrate animals, biohazards, and/or select agents**

Nothing to Report.

6. PRODUCTS:

➢ Publications, conference papers, and presentations

A. Scientific Publications

Bhat V, Lefebvre C, Goodale D, Rodriguez-Torres M, **Allan AL**. Isolation and functional assessment of human breast cancer stem cells from cell and tissue samples. 2020 *JoVE,* In press. Federal support acknowledged: Yes.

B. Scientific Presentations

Goodale, D., Xia, Y., Postenka, C., and **Allan, A.L.** Knockout of lung-derived osteopontin or selectins reduces metastatic colonization in an *ex vivo* model of breast cancer lung metastasis. 2019 Canadian Cancer Research Conference, November 2019, Ottawa Canada. Federal support acknowledged: Yes.

Allan, A.L. Role of the lung microenvironment in mediating breast cancer metastasis: a balance between the "seed" and the "soil". Department of Anatomy & Cell Biology Seminar Series, Schulich School of Medicine & Dentistry, Western University, London ON, January 2020. Federal support acknowledged: Yes.

➢ Website(s) or other Internet site(s)

Nothing to Report.

➢ Technologies or techniques

Nothing to Report.

➢ Inventions, patent applications, and/or licenses

Nothing to Report.

➢ Other Products

Nothing to Report.

7. PARTICIPANTS & OTHER COLLABORATING ORGANIZATIONS

➢ What individuals have worked on the project?

Name:	Alison Allan
Project Role:	PD/PI
Researcher Identifier:	Scopus Author ID: 8966957100
Nearest person month worked:	3

Contribution to Project:	Dr. Allan has performed work in the area of overseeing and managing all aspects of the project.
Funding Support:	Salary support from the University of Western Ontario (65%) and the Breast Cancer Society of Canada (35%).

Name:	Ying Xia
Project Role:	Research Associate
Researcher Identifier:	Scopus Author ID: 57190123286
Nearest person month worked:	5.4
Contribution to Project:	Dr. Xia performed work in the area of *in vitro* and *ex vivo* functional and mechanistic studies of breast cancer metastatic behavior, and in daily supervision of graduate and undergraduate research students. She completed her work in the Allan lab in mid-February 2020 and moved to a different lab at Western University to take up a new position.
Funding Support:	Salary support from this project (45%) and Western University (65%)

Name:	David Goodale
Project Role:	Technician
Researcher Identifier:	Scopus Author ID: 36897019500
Nearest person month worked:	12
Contribution to Project:	Mr. Goodale has performed work in the area of animal husbandry, animal studies (*in vivo* and *ex vivo*) of breast cancer metastatic behavior, and in daily management of Dr. Allan's lab.
Funding Support:	Salary support from this project (100%).

Name:	Carl Postenka
Project Role:	Technician
Researcher Identifier:	Scopus Author ID: 6506850250
Nearest person month worked:	2.4
Contribution to Project:	Mr. Postenka has performed work in the area of animal husbandry, histopathology, and in daily maintenance/upkeep of Dr. Allan's lab.

Funding Support:	Salary support from this project (20%), and 80% from the Translational Breast Cancer Research Unit at the London Health Sciences Centre.

Name:	Raimar Loebenberg
Project Role:	Co-Investigator
Researcher Identifier:	Scopus Author ID: 6602898019
Nearest person month worked:	1.5
Contribution to Project:	Dr. Loebenberg has performed work in the area of overseeing the drug formulation aspects of the project at the University of Alberta (Sub-Award site).
Funding Support:	Salary support from the University of Alberta (100%).

Name:	Vijay Somayaji
Project Role:	Manager
Researcher Identifier:	Scopus Author ID: 6603256858
Nearest person month worked:	3.6
Contribution to Project:	Dr. Somayaji has performed work in the area of drug formulation studies, daily supervision of graduate students, and in daily management of Dr. Loebenberg's lab.
Funding Support:	Salary support from this project (30%) and from the University of Alberta (70%).

Name:	Daniela Amaral-Silva
Project Role:	Graduate Student
Researcher Identifier:	Not applicable
Nearest person month worked:	6.5
Contribution to Project:	Ms. Amaral-Silva has performed work in the area of drug formulation studies.
Funding Support:	Salary support from this project (0%); supported by external graduate student awards (100%).

- **Has there been a change in the active other support of the PD/PI(s) or senior/key personnel since the last reporting period?**

Dr. Alison Allan, PD/PI:

- New grant (0% overlap with the current project)

Title of Grant:	A phase III randomized controlled trial and economic evaluation of Stereotactic Ablative Radiotherapy (SABR) for Comprehensive treatment of OligoMETastatic (1-3 metastases) cancer: SABR-COMET-3
Source:	Canadian Institutes of Health Research; Project Grant Program
Amount:	$699,380 total (CAD)
Dates of Project:	2020-2026
Name of P.I.:	Robert Olson (*Nominated PI*); David Palma, **Alison L. Allan**, Stuart Peacock, Scott Tyldesley (*Co-PIs*)
Co-Applicants:	Alanah Bergman, Mitchell Liu, Alex Louie, Liam Mulroy, Helen McTaggart-Cowan, Devin Schellenberg, Senthi Sashendra, Andrew Warner

- **What other organizations were involved as partners?**

Nothing to Report.

8. SPECIAL REPORTING REQUIREMENTS

- **Collaborative Awards:**

Not Applicable.

- **Quad Charts:**

Not Applicable.

9. APPENDICES:

Bhat V, Lefebvre C, Goodale D, Rodriguez-Torres M, **Allan AL**. Isolation and functional assessment of human breast cancer stem cells from cell and tissue samples. 2020 *JoVE,* In press (*accepted manuscript appended*). Federal support acknowledged: Yes.

jove JOURNAL OF VISUALIZED EXPERIMENTS
1 Alewife Center #200
Cambridge, MA 02140
tel. 617.945.9051
www.jove.com

TITLE:

Isolation and functional assessment of human breast cancer stem cells from cell and tissue samples

AUTHORS AND AFFILIATIONS:

Vasudeva Bhat[1,2], Cory Lefebvre[1,2], David Goodale[1], Mauricio Rodriguez-Torres[1,2], and Alison L. Allan[1,2,3,4]

[1]London Regional Cancer Program, London, Ontario CANADA
[2]Department of Anatomy & Cell Biology, Western University, London, Ontario CANADA
[3]Department of Oncology, Western University, London, Ontario CANADA
[4]Lawson Health Research Institute, London, Ontario CANADA

Email address of co-authors

Vasudeva Bhat	vbhat@uwo.ca
Cory Lefebvre	clefebvre6@uwo.ca
David Goodale	david.goodale@lhsc.on.ca
Mauricio Rodriguez-Torres	rodrimauricio@gmail.com

Corresponding author

Alison L. Allan	alison.allan@lhsc.on.ca

KEYWORDS:

Breast cancer stem cell (BCSC), fluorescence-activated cell sorting (FACS), colony forming assay, mammosphere assay, 3D culture model, *in vivo* tumor model

SUMMARY:

This experimental protocol describes the isolation of BCSCs from breast cancer cell and tissue samples as well as the *in vitro* and *in vivo* assays that can be used to assess BCSC phenotype and function.

ABSTRACT:

Breast cancer stem cells (BCSCs) are cancer cells with inherited or acquired stem cell-like characteristics. Despite their low frequency, they are major contributors to breast cancer initiation, relapse, metastasis and therapy resistance. It is imperative to understand the biology of breast cancer stem cells in order to identify novel therapeutic targets to treat breast cancer. Breast cancer stem cells are isolated and characterized based on expression of unique cell surface markers such as CD44, CD24 and enzymatic activity of aldehyde dehydrogenase (ALDH). These $ALDH^{high}CD44^{+}CD24^{-}$ cells constitute the BCSC population and can be isolated by fluorescence-activated cell sorting (FACS) for downstream functional studies. Depending on the scientific question, different *in vitro* and *in vivo* methods can be used to assess the functional characteristics of BCSCs. Here we provide a detailed experimental protocol for isolation of human BCSCs from both heterogenous populations of breast cancer cells as well as primary tumor tissue obtained from breast cancer patients. In addition, we highlight downstream *in vitro* and *in vivo*

functional assays including colony forming assays, mammosphere assays, 3D culture models and tumor xenograft assays that can be used to assess BCSC function.

INTRODUCTION:

Understanding the cellular and molecular mechanisms of human breast cancer stem cells (BCSCs) is crucial for addressing the challenges encountered in breast cancer treatment. The emergence of the BCSC concept dates back to the early 21st century, where a small population of $CD44^{+}CD24^{-/low}$ breast cancer cells were found to be capable of generating heterogenous tumors in mice[1,2]. Subsequently, it was observed that human breast cancer cells with high enzymatic activity of aldehyde dehydrogenase ($ALDH^{high}$) also displayed similar stem cell-like properties[3]. These BCSCs represent a small population of cells capable of self-renewal and differentiation, contributing to the heterogenous nature of bulk tumors[1-3]. Accumulating evidence suggest that alterations in evolutionarily conserved signaling pathways drive BCSC survival and maintenance[4-14]. In addition, the cell extrinsic microenvironment has been shown to play a pivotal role in dictating different BCSC functions[15-17]. These molecular pathways and the external factors regulating BCSC function contribute to breast cancer relapse, metastasis[18] and development of resistance to therapies[19-21], with the residual existence of BCSCs post-treatment posing a major challenge to the overall survival of breast cancer patients[22,23]. Pre-clinical evaluation of these factors is therefore very important for identifying BCSC-targeting therapies that could be beneficial for achieving better treatment outcomes and improved overall survival in breast cancer patients.

Several *in vitro* human breast cancer cell line models and *in vivo* human xenograft models have been used to characterize BCSCs[24-29]. The ability of cell lines to continuously repopulate after every successive passage makes these an ideal model system to perform omics-based and pharmacogenomic studies. However, cell lines often fail to recapitulate the heterogeneity observed in patient samples. Hence, it is important to compliment cell line data with patient-derived samples. Isolation of BCSCs in their purest form is important for enabling detailed characterization of BCSCs. Achieving this purity depends on the selection of phenotypic markers that are specific to BCSCs. Currently, the $ALDH^{high}CD44^{+}CD24^{-}$ cell phenotype is most commonly used to distinguish and isolate human BCSCs from bulk breast cancer cell populations using fluorescence activated cell sorting (FACS) for maximum purity[1,3,26]. Furthermore, the properties of isolated BCSCs such as self-renewal, proliferation, and differentiation can be evaluated using *in vitro* and *in vivo* techniques.

For example, *in vitro* colony forming assays can be used to assess the ability of a single cell to self-renew to form a colony of 50 cells or more in presence of different treatment conditions[30]. Mammosphere assays can also be used to assess the self-renewal potential of breast cancer cells under anchorage-independent conditions. This assay measures the ability of single cells to generate and grow as spheres (mixture of BCSCs and non-BCSCs) at each successive passage in serum-free non-adherent culture conditions[31]. Additionally, 3-Dimensional (3D) culture models can be used to assess BCSC function, including cell-cell and cell-matrix interactions that closely recapitulate the *in vivo* microenvironment and allow investigation of the activity of potential BCSC-targeted therapies[32]. Despite the diverse applications of *in vitro* models, it is difficult to model the complexity of *in vivo* conditions using only *in vitro* assays. This challenge can be

overcome by use of mouse xenograft models to evaluate BCSC behavior *in vivo*. In particular, such models serve as an ideal system for assessing breast cancer metastasis[33], investigating interactions with the microenvironment during disease progression[34], *in vivo* imaging[35], and for predicting patient-specific toxicity and efficacy of antitumor agents[34].

This protocol provides a detailed description for the isolation of human $ALDH^{high}CD44^{+}CD24^{-}$ BCSCs at maximum purity from bulk populations of heterogenous breast cancer cells. We also provide a detailed description of three *in vitro* techniques (colony forming assay, mammosphere assay, and 3D culture model) and an *in vivo* tumor xenograft assay that can be used to assess different functions of BCSCs. These methods would be appropriate for use by investigators interested in isolating and characterizing BCSCs from human breast cancer cell lines or primary-patient derived breast cancer cells and tumor tissue for the purposes of understanding BCSC biology and/or investigating novel BCSC-targeting therapies.

PROTOCOL:

1. Preparation- cell lines

1.1 Perform all cell culture and staining procedures under sterile conditions in a biosafety cabinet. Use sterile cell culture dishes/flasks and reagents.

1.2 Maintain human breast cancer cells at 37 °C with 5% CO_2 in defined media supplemented with fetal bovine serum (FBS) and necessary growth factors specific to each cell line.

1.3 Maintain mouse NIH3T3 fibroblast cell cultures (for use in colony forming assays) at 37 °C with 5% CO_2 in Dulbecco's Modified Eagle's Medium (DMEM) supplemented with 10% FBS.

1.4 For all cultures, replenish the old media every 2-3 days with fresh media. Once the cultures reach 75-80% confluency, subculture into multiple sterile cell culture flasks.

2. Preparation- breast cancer tumor tissue

2.1 Collect the patient-derived surgical or biopsy samples directly from consenting breast cancer patients under a human ethics protocol approved by the institutional ethics board.

2.2 Subsequently, collect and generate tumor tissue from patient-derived xenograft models using mice under an animal ethics protocol approved by the institutional animal care committee.

2.3 Collect all tumor tissues under sterile conditions into a 50 mL sterile conical tube containing 30 mL DMEM:F12 media, keep on ice, and process the samples as described below within 2 hr of collection.

3. Generation of single cell suspensions of breast cancer cells

3.1 Aspirate media from the flask containing a monolayer of breast cancer cells that is 60-80% confluent (cell lines of your choice). Wash the cells with 1x phosphate buffered saline (PBS). Aspirate PBS and add appropriate cell dissociation solution (e.g. Trypsin:EDTA; just enough to cover the monolayer of cells) and incubate for 5 min at room temperature (recommended) or at 37 °C.

3.2 Add 5 mL of culture media to neutralize the activity of cell dissociation solution.

3.3 Transfer the resulting dissociated cell solution to a 50 ml conical tube and centrifuge at 1000 x *g* for 5 min.

3.4 Discard supernatant and resuspended the cell pellet in 5 mL of 1x PBS. Count the cells using hemocytometer and microscope.
Note1: observe for cell clumping in the hemocytometer. Repeat cell dissociation step if single cell suspension has not formed.
3.5 After cell counting, re-centrifuge the cell suspension at 1000 x *g* for 5 min, discard supernatant, and resuspend the cell pellet in ALDH substrate buffer at a concentration of 1 x 10^6 cells/mL.

4. Generation of single cell suspension from tissue samples

4.1 Mince the tumor tissue with surgical blades using a crisscross technique to obtain smaller pieces of approximately 1 mm in size. Transfer the tissue pieces into a fresh 50 mL conical tube containing 10 mL dissociation buffer. Seal the conical tube with parafilm and incubate at 37 °C in a shaker incubator for 40 min.
Note 2: If you don't have a shaker incubator, place the tube in a 37 °C water bath and mix the tube by vortexing every 5-10 min.
4.2 Pellet the digested tissue by centrifuging sample at 530 x *g* for 5 min. Discard the supernatant and add 5 mL of trypsin. Pipette up and down using 1 mL pipette (set to 750 µL mark) to disrupt the pellet and incubate in a 37°C water bath for 5 min. After incubation, pipette up and down vigorously to release single cells.
4.3 Top up the total volume in the tube to 25 mL with DMEM:F12 media and centrifuge at 1000 x *g* for 5 min. Discard the supernatant and resuspend the pellet in 1 mL of dispase + DNase. Incubate in a 37 °C water bath for 5 min.
4.4 Top up the total volume in the tube to 10 mL with PBS. Mix by pipetting up and down, pass the resulting cell suspension through a 40 µm cell strainer attached to a fresh 50 mL conical tube. Centrifuge at 1000 x *g* for 5 min.
4.5 Discard supernatant and resuspend the cell pellet in 5 mL of 1x PBS. Count the cells and complete preparation of the cell suspension as described in steps 3.4 and 3.5.

5. Isolation of breast cancer stem cells (BCSCs)

5.1 Label flow tubes for the unstained control, single cell staining controls (DEAB control, ALDH, CD44-PE, CD24-PE-Cy7, 7AAD), the negative control tube (stained with DEAB, CD44-PE, CD24-PE-Cy7 and 7AAD), fluorescent minus one (FMO) control and the 'sort' tube (stained with ALDH, CD44, CD24 and 7AAD).
5.2 Transfer 500 µL (0.5 x 10^6 cells) of the cell suspensions from step 3.5 or step 4.5 to each tube that is labelled cells only, CD44, CD24 and 7AAD. Place the tubes on ice until use.
5.3 Transfer 2 mL of sample (2 x 10^6 cells) to respective 'ALDH' tube. Add 5 µL of DEAB to the 'DEAB control' and 'negative control' tubes and cap it tightly. Add 10 µL of ALDH substrate to the 'ALDH' tube, mix well by vortexing, and immediately transfer 500 µL to corresponding 'DEAB control' and 'negative control' tube. Recap the 'DEAB control', 'negative control' and 'ALDH tubes' and incubate at 37 °C for 30-60 min (do not exceed 60 min).
Note 3: The optimal incubation time may require optimization depending on the cell line. Always protect the ALDH substrate and the tubes containing stained cells from light.
5.4 Following incubation, centrifuge all samples for 5 min at 250 x *g*. Resuspend the cells in 500

μL of ALDH substrate buffer. Add manufacturer-recommended or user-optimized concentration of anti-CD44-PE and anti-CD24-PE-Cy7 antibody cocktail and incubate at 4°C for 30 min. Add anti-CD44-PE and anti-CD24-PE-Cy7 antibodies to respective 'CD44' and 'CD24' labelled tubes.

5.5 Following incubation, centrifuge all samples at 250 x *g* for 5 min. Resuspend the cells in 500 μL of ALDH substrate buffer. Incubate the 'negative control' tube, 'Sort tube' and the '7ADD' tube with 7AAD (suggested concentration: 0.25 μg/1 x 10^6 cells) for 10 min on ice.

Note 4: The ALDH activity is detected in the green fluorescent channel, therefore a fluorochrome with a different compatible emission spectrum should be used. Where spectral overlap is observed during multi-parameter flow cytometry, single color controls and FMO control should be used as a guide to allow compensation between fluorochromes to minimize the spill over of fluorescent signal into other channels.

5.6 Set up the analysis protocol on the FACS instrument in preparation for sample analysis. Create scatter plots (forward vs side scatter, forward scatter vs fluorescent channels).

5.7 Using the unstained control, adjust the photomultiplier to separate debris from whole cell population and adjust the fluorescent voltage to move the whole cell population around the first log scale (10^1). Using the DEAB control, move the whole cell population within the second log scale (10^2) by adjusting the green fluorescent voltage channel.

5.8 Analyze all the single staining controls first (ALDH, CD44-PE, CD24-PE-Cy7) and 7AAD and FMO control, adjusting the voltage to separate stained from unstained cells and to minimize the spillage of fluorescent signals into other channels.

5.9 Gate on the positive population for each single stained cell sample. Using the negative control tube, gate for viability (7AAD negative), $ALDH^{low}$ and $ALDH^{high}$ cell populations (representative gating strategy shown in **Figure 1B**).

5.10 Analyze multiparameter stained samples of interest to isolate BCSCs. Using the viable $ALDH^{low}$ and $ALDH^{high}$ gates, select for $CD44^+CD24^-$ (BCSC) and $CD44^-CD24^-$ (non-BCSC) cell population respectively (**Figure 1B**).

5.11 Collect viable BCSCs and non-BCSCs in collection media in sterile collection tubes (populations from two representative cell lines shown in **Figure 2A&B**). Use sorted cells for downstream *in vitro* and *in vivo* assays as described below.

Note 5: In addition to in vitro and in vivo assays described below, BCSCs can be validated by measuring the expression of pluripotent markers such as SOX2, OCT4 and NANOG via standard immunoblotting techniques.

(*Insert Figures 1, 2 here*)

6. Colony forming assay

6.1 Resuspend the cells of interest (sorted cells from step 5.11 or unsorted cells from steps 3.5 or 4.5) in complete media.

6.2 Label three flow tubes for 1 x 10^2, 2 x 10^2 and 5 x 10^2 cells. Add 2 mL of complete media and transfer the appropriate cell number (sorted from step 5.11 or unsorted cells from steps 3.5 or 4.5) in respective tubes. Mix the cell solutions thoroughly by pipetting it up and down 5 times.

6.3 Plate the cells in a 6-well plate and distribute the cell suspension by gently swirling the plates

to obtain uniform distribution of cells.

6.4 Incubate the plates in a 37 °C, 5% CO_2 incubator until colonies appear (where colonies = ≥50 cells per colony). Carefully replenish media twice a week without disturbing colony formation.

6.5 Aspirate media and wash once with 1 mL PBS. Add 0.5 mL of 0.05% crystal violet solution into each well and incubate the plate for 30 minutes. Remove excess crystal violet stain by washing with 2 mL of water. Repeat the washing step until background staining has been removed.

6.6 Using a microscope at 4x and 10x magnification, count and record the total number of colonies generated (representative images shown in **Figure 3A**).

6.7 Calculate the frequency of colony formation as follows: Frequency (%) = (# of colonies formed/number of cells seeded) x 100. For example, if 25 colonies are generated from 1 x 10^2 cells, then the Frequency of colony formation is, Frequency = (25/100) x100 = 25%.

4.1 Alternatively, replace steps 6.1 to 6.4 with an alternate method involving co-culture with fibroblasts, which provide a microenvironmental support for BCSCs through production of necessary growth and survival factors.

6.9 Pre-coat cell 60mm culture dishes with type I bovine collagen (1 in 30 dilution of 3 mg/mL collagen). Allow collagen to polymerize for 30 min in a 37 °C incubator. Aspirate the unpolymerized collagen and wash the plate twice with 1x PBS. Cover the collagen-coated plate with 1 mL PBS and set it aside at room temperature until use.

6.10 Label three flow tubes for 1 x 10^3, 5 x 10^3 and 1 x 10^4 cells. Add 4 mL of colony forming assay media and transfer the appropriate number of cells (sorted from step 5.11 or unsorted cells from steps 3.5 or 4.5) into the respective tubes. Add irradiated mouse NIH3T3 fibroblasts (4 x 10^4 cells/mL of media). Mix cell solutions thoroughly by pipetting it up and down 5 times.

6.11 Aspirate the PBS from the collagen-coated culture dish from step 6.1 and plate the cell mixture onto each of the cell culture plates as described in step 6.3.

6.12 Incubate the plates in a 37 °C, 5% CO_2 incubator and leave them undisturbed for 7-10 days or until colonies form, without replenishing the media. Count and record the total number of colonies generated as described in steps 6.6 and 6.7.

7. Mammosphere assay

7.1 Resuspend the cells of interest (sorted cells from step 5.11 or unsorted cells from steps 3.5 or 4.5) in complete mammosphere media and plate cells at a seeding density of 5 x 10^2 cells/cm^2 area in a 96 well ultra-low attachment cell culture plate.

Note 6: Cell seeding density should be optimized for different cell lines.

7.2 Incubate the culture plates for 5-10 days in a 37 °C incubator with 5% CO_2. Carefully replenish media twice a week without disturbing mammosphere formation.

7.3 After incubation, count the number of mammospheres generated in each well using a microscope; where mammospheres are defined as breast cancer cell clusters greater than 100 μm in diameter (representative images shown in **Figure 3B**).

7.4 Calculate the mammosphere formation efficiency (MEF) as follows: MFE (%) = (number of mammospheres per well)/ (number of cells seeded per well) x 100 (i.e. if 5 mammospheres are generated by 1 x 10^2 cells in a well, then MFE = (5/100) x 100 = 5%).

7.5 To subculture mammospheres, carefully transfer the media containing mammospheres

content into a fresh 50 mL conical tube and centrifuge media at 1000 x *g* for 5 min. Carefully remove supernatant, resuspend cell pellet in 500 μL of trypsin, and incubate for 5 min at room temperature.

7.6 Discard the supernatant and resuspend the pellet in 1 mL of complete mammosphere media. Count the cells using a hemocytometer and re-plate the cells in an ultra-low attachment cell culture plate as described in step 7.1.

Note 7: In addition to sub-culturing, the mammosphere-derived cells can be also analyzed further by FACS to assess BCSC phenotype and/or obtain pure populations of BCSCs for other downstream assays.

7.7 To determine the number of mammosphere-initiating cells contained within your cell populations, use an alternate method involving sphere limiting dilution analysis (SLDA). Plate cells in serial dilutions of high to low cell numbers in a 96 well ultra-low attachment cell culture plate, with the highest dilution resulting in less than one cell per well.

7.8 Incubate the culture plate for 10-14 days in a 37 °C incubator with 5% CO_2 and leave them undisturbed to avoid cell aggregation.

7.9 After incubation, count the number of mammospheres generated in each well using a microscope; where mammospheres are defined as breast cancer cell clusters greater than 100 μm in diameter. Calculate the sphere-initiating frequency and significance using Extreme Limiting Dilution Analysis (ELDA) online software (http://bioinf.wehi.edu.au/software/elda/).

8. 3D culture model

8.1 Depending on the experimental question, use basement membrane extract (BME) with or without growth factors (reduced). In order to evaluate the effect of individual growth factor on cancer cells, use growth factor reduced BME. It also helps in minimizing the non-specific effects of endogenous growth factors present in BME.

Note 8: BME solidifies above 10 °C. Always keep BME on ice even during the thawing step.

8.2 Carefully add 50 μL of BME per well in a 96-well plate without creating air bubbles and allow it to polymerize at 37 °C for 1 h. After 10 min of incubation, add PBS to avoid drying of the gel layer.

8.3 Resuspend the sorted cells from step 5.11 or unsorted cells from steps 3.5 or 4.5 at a concentration of 5 x 10^3 to 5 x 10^4/200 μL in 3D culture media.

8.4 Once the BME has polymerized, remove PBS, add 200 μL of cell suspension to each well and incubate in 37 °C incubator with 5% CO_2. Add PBS to the surrounding wells to avoid evaporation of the media.

Note 9: The optimal number of cells for plating should be determined prior to setting of the experiment. Depending on the experimental question, BCSCs can be cultured alone or with other cells types (fibroblasts/endothelial/immune cells etc.).

8.6 Add fresh media to the culture plates twice weekly. Maintain cultures for 10-14 days prior to analyzing the formation of organoids (representative images shown in **Figure 3C**).

8.7 For sub-culturing, carefully aspirate the media and add 200 μL of dispase to each well containing cells. Incubate the plate in a 37 °C incubator for 1 h. Halfway through the incubation period (30 min), take out the plate, gently pipette the dispase solution up and

down 5 times, and place back in the incubator for a further 30 min.

8.8 After 1 h, transfer the dissociated cell solution to a flow tube. Wash the well with 1x PBS containing 2% FBS (fPBS) and transfer it to the flow tube. Centrifuge the tube at 1000 x *g* for 5 min. Carefully aspirate the supernatant and add 500 µL of trypsin, incubate at 37 °C for 5 min. Inactivate trypsin by adding equal amount of fPBS and centrifuge at 1000 x *g* for 5 min.

8.9 Discard the supernatant and resuspend the pellet in 1 mL of 3D culture media. Count the cells and re-plate required number of cells in the BME as in steps 8.2 to 8.4.

Note 10: Multiple wells can be pooled to further analyze or sort the cell population of interest.

(Insert Figure 3 here)

9. *In vivo* xenograft model

9.1 Perform animal experiments under an animal ethics protocol approved by the institutional animal care committee.

9.2 In order to determine the tumor initiation capacity of breast cancer stem cells, prepare cells (sorted population from step 5.7 or unsorted populations from steps 3.5 or 4.5) using a limiting dilution approach. Serially dilute cells in PBS using between 1 and 5 different dilution groups, with doses as low as 0.01-0.2 x 10^2 cells/100 µL and as high as 1 x 10^6 cells/100 µL.

Note 11: Unsorted/whole population cells can be used as a control. The number of dilution groups used will depend on the desired scientific outcome (e.g. if only testing tumorgenicity then 1 group at a higher cell number may be used, whereas when calculating tumor-initiating capacity, it is optimal to test 5 limiting dilution doses).

9.3 To generate xenograft models from human breast cancer cells, use immunocompromised female mice (athymic nude [*nu/nu*], nonobese diabetic/severe combined immunodeficient [NOD/SCID] or NOD/SCID IL2γ [NGS] strains).

Note 12: Although a minimum of 4 animals per group can be used, 8-12 animals per group is recommended to obtain robust results particularly for limiting dilution analysis.

9.4 Perform standard mammary fat pad (MFP) injections using 100 µL/mouse of each cell preparation, under sterile conditions in a biosafety cabinet.

Note 13: For optimal breast tumor growth and spontaneous metastasis to distant organs, the thoracic MFP is recommended. Alternatively, the inguinal MFP can also be used.

9.5 Post-injection, monitor the mice on a daily basis for general health and tumor growth at the site of injection. Upon detection of a palpable tumor, begin measuring the tumor size by calipers in two perpendicular dimensions and record weekly until endpoint.

Note 14: The experimental end point is determined based on the regulations laid out the institutional animal ethics protocol; typically, endpoint by euthanasia is usually required once tumor volumes reach 1500 mm^3. For BCSC populations and/or higher cell doses (e.g. >1 x 104 cells), this endpoint will likely be reached within 4-8 weeks of MFP injection. For very low cell doses and/or non-BCSC cell populations, tumor growth should be allowed to progress for up to 8 months post-injection.

9.6 From these measurements, calculate the tumor volume using the following formula: Volume in mm^3 = 0.52 x $(width)^2$ x length. If using a limiting dilution approach, calculate tumor-initiating capacity and significance using ELDA online software

(http://bioinf.wehi.edu.au/software/elda/).

9.7 Alternatively, to humanely extend the endpoint, surgically remove primary tumors and continue to monitor mice for health and/or development of spontaneous metastasis in distant organs. Use resected tumor tissue for the generation of serial xenotransplants.

9.8 At endpoint, harvest tissue from primary tumors and distant organs (lymph nodes, lung, liver, brain, bone) and carry out histopathological and/or immunohistochemical analysis or dissociated the tumor tissue and use in the *in vitro* assays described in sections 6-8.

REPRESENTATIVE RESULTS:

The described protocol allows isolation of human BCSCs from a heterogenous population of breast cancer cells, either from cell lines or from dissociated tumor tissue. For any given cell line or tissue sample, it is crucial to generate a uniform single cell suspension to isolate BCSCs at maximum purity as contaminating non-BCSC populations could result in variable cellular responses, especially if the study aim is to evaluate the efficacy of therapeutic agents targeting BCSCs. Application of a stringent sorting strategy will minimize the presence of contaminating non-BCSCs and result in the ability to collect the proportion of breast cancer cells with stem cell-like characteristics that display a cellular phenotype that distinguishes them from bulk population of cancer cells. Human breast cancer cells that exhibit enhanced ALDH enzymatic activity, express high levels of the cell surface marker CD44, and low/negative expression of CD24 have an $ALDH^{high}CD44^{+}CD24^{-}$ phenotype and can be classified as BCSCs. The proportion of BCSCs within the bulk population can vary between cell lines or patients (**Figure 2**), and often depends on disease stage, with more aggressive breast cancer usually displaying a higher proportion of BCSCs[26,36,37].

Isolated BCSCs can be used to perform different *in vitro* and *in vivo* assays where their behavior and function can be compared to that of the bulk and/or non-BCSC populations. For example, the ability of a single breast cancer cell to self-renew and generate colonies of 50 cells can be assessed by colony-forming assays (**Figure 3A**). The ability of BCSCs to self-renew under anchorage-independent experimental conditions can be assessed by mammosphere assays, where variable sphere number, size, and sphere-initiating capacity can be analyzed and correlated with the presence and function of BCSCs (**Figure 3B**). It is important to determine the seeding cell densities for different breast cancer cell lines or breast tumor samples to obtain optimal results. This is particularly important when performing SLDA, as higher cell densities could lead to cell aggregation resulting in misinterpretation of cellular activity.

Culturing breast cancer cells in BME allows BCSCs to form 3D structures that recapitulate *in vivo* conditions (**Figure 3C**). 3D culture of breast cancer cells in the presence of other microenvironmental cell types such as fibroblasts, endothelial cells, and/or immune cells has the added capacity for investigating the role of microenvironment in 3D growth of BCSCs[38,39]. The specific cell numbers required to generate 3D organoids may vary depending on the cell line or patient tumor source, and thus it is important to optimize the culture conditions and cell numbers prior to any large-scale experiments.

Finally, *in vivo* mouse xenograft models can be used to understand the differences in growth

(**Figure 4**) self-renewal, differentiation and/or tumor-initiating ability of BCSCs *in vivo* compared to non-BCSCs or bulk cell populations. Often, the *in vitro* cellular responses observed in the presence of exogenous factors or therapeutic agents is not representative of *in vivo* setting, suggesting that *in vitro* observation should be complimented with *in vivo* studies whenever feasible. Using *in vivo* xenograft models, the cellular heterogeneity and tumor architecture is preserved and thus these models can serve as a system that closely mimics the microenvironment in human patients. *In vivo* LDA can be performed to determine the proportion of tumor-initiating cells in a given mixed population of cancer cells (BCSCs or non-BCSCs)[40,41]. The range of cell dilutions used should be optimized and will depend on the frequency of initiating cells in the cell population of interest. Ideally these dilutions should include doses that result in 100% tumor formation, down to cell doses with no tumor formation and a reasonable range in between. The frequency of tumor-initiating cells in primary samples can be variable, and in instances where breast tumors have very low numbers or heterogenous populations of tumor-initiating cells, performing LDA can be particularly challenging[42]. In these cases, injecting larger number of cells would be more appropriate for understanding breast cancer biology.

(Insert Figure 4 here)

FIGURE AND TABLE LEGENDS:

Figure 1: **FACS gating strategy for isolation of BCSCs from breast cancer cell lines and tissue samples**. (A) Flowchart describing the procedure of BCSC isolation. (B)Representative FACS plots showing the sort strategy used to isolate viable BCSCs and non-BCSCs from a heterogenous pool of cells. MDA-MB-231 human breast cancer cells are concurrently labeled with 7-AAD, CD44-APC, CD24-PE and the ALDH substrate. Cell subsets were isolated using a four-color protocol on a FACS ARIA III (Becton Dickinson). Cells are selected based on expected light scatter, then for singlets, and viability based on 7-AAD exclusion. Cells are then analyzed for ALDH activity and the top 20% most positive are selected as the $ALDH^{high}$ population, while the bottom 20% of cells with the lowest ALDH activity were deemed to be $ALDH^{low}$. Finally, 50% of the $ALDH^{low}$ cells are further selected based on a $CD44^{low/-}CD24^{+}$ phenotype, and 50% of the $ALDH^{high}$ cells are selected based on $CD44^{+}CD24^{-}$ phenotype. This figure has been adapted from Chu et al, 2014[17].

Figure 2: **BCSCs proportions are variable in different breast cancer cell lines**. Representative image showing the differential proportion of BCSCs and non-BCSCs in (A) SUM159 and (B) MDA-MD-468 triple negative breast cancer cell lines following labelling and sorting as described in Figure 1.

Figure 3: ***In vitro* assays to assess BCSC cell function**. *In vitro* assays were performed as described in protocol sections 6.1 to 6.5 (A), 7.1 to 7.4 (B), or 81. to 8.4 + 8.6 (C). (A) Representative image showing the colonies generated by MDA-MB-231 human breast cancer cells; (B) Representative images showing mammosphere formation by MCF7, SUM159, or MDA-MB-468 human cell lines as well as patient-derived LRCP17 breast cancer cells. (C) Representative images showing the 3D structures formed by MCF7 and MDA-MB-231 breast cancer cells in 3D cultures models.

Figure 4: ***In vivo* xenograft assays to assess BCSC function.** MDA-MB-231 breast cancer cells were isolated by FACS as described in Figure 1 and injected into the right thoracic mammary fat pad of female NSG mice as described in protocol sections 9.1 to 9.8 ($5x10^5$ cells/mouse; 4 mice/cell population). Primary breast tumor growth kinetics are shown for $ALDH^{hi}CD44^{+}CD24^{-}$ (■) versus $ALDH^{low}CD44^{low/-}CD24^{+}$ (□) populations. Data represented as the mean ± S.E.M. * = significantly different tumor size than respective $ALDH^{low}CD44^{low/-}$ subsets at the same time-point ($P < 0.05$). This figure has been adapted from Croker et al., 2009[26].

DISCUSSION:

Breast cancer metastasis and resistance to therapy have become major cause of mortality in women worldwide. The existence of a sub-population of breast cancer stem cells (BCSCs) contributes to enhanced metastasis[26,43-46] and therapy resistance[21,47,48]. Therefore, the focus of future treatments should aim at eradicating BCSCs to achieve better treatment outcomes, and this requires accurate methods for isolating and characterizing the functional characteristics of BCSCs using both *in vitro* and *in vivo* methods.

Immortalized cell lines derived from different subtypes of breast cancer have proven to be feasible models to study breast cancer biology including the isolation and characterization of BCSCs[26,49,50]. The high proliferative capacity and unlimited expansion ability of cell lines provides an ideal model system for performing studies that are highly reproducible and technically straightforward. However, due to the clonal origin of cell lines, they may fail to recapitulate the heterogeneity exhibited by different patients and/or by cancer cells within tumor tissue. In addition, genetic alterations can be acquired during serial passaging of cell lines and may induce genotypic or phenotypic changes that can confound experimental results[51]. In contrast, primary patient-derived cells, despite their limited proliferative and expansion ability, may provide a more accurate model to that observed *in viv*o. However, such samples may be more difficult to acquire and be more technically challenging to work with. All of these factors should be considered when choosing a starting model system with which to isolate and characterize BCSCs.

FACS is a commonly used technique to isolate cells of interest based on cell surface marker expression[52,53]. Based on cell surface antigens (CD44 and CD24) and ALDH enzymatic activity, human BCSCs can be isolated at high purity from both breast cancer cell lines and tumor tissues[1,2]. The sorting efficiency determines the purity of sorted sample, and it is recommended that users analyze a small portion of sorted sample incubated with viability dye to check the efficiency of sorting[53,54]. The sorting efficiency can be confounded by many factors including the presence of cell clumps, a high number of dead or dying cells, improper compensation of the fluorochromes and/or damage to cell surface antigens due to sensitivity to trypsin or collagenase during pre-sorting dissociation steps[53-55]. Therefore, generation of a proper single cell suspension and use of appropriate cell dissociation techniques will increase the sorting efficiency. While performing multiparameter cell sorting, it is important to choose fluorochromes that minimizes spectral overlap. In some cases, where spectral overlap cannot be avoided, a control that contains all the fluorochromes except one (fluorescence minus one, FMO) should be used to minimize the spillover of fluorescent signals into other channels[54]. Alternatively, the spectral overlap can reduced be by immunomagnetically isolating cell populations prior to final FACS

isolation of cells of interest[56].

In vitro assays such as the colony-forming and mammosphere assays described in this protocol have been extensively used to study the self-renewal and proliferative ability of BCSCs[57-61]. Additionally, these assays can be used to assess the activity of different therapeutic drugs on BCSC function. Several evolutionarily conserved signaling pathways have been implemented in BCSC maintenance[62], and both colony-forming[63-65] and mammosphere assays[63,66] have been used to assess the value of therapeutic disruption of these pathways as an intervention to block BCSC intrinsic signaling and reduce BCSC activity and disease progression. Colony forming assay using primary cells can be challenging due to low cell density, variation between samples and lack of its adaptability to isolated *in vitro* conditions. These challenges can be overcome by culturing BCSCs on a soft agar layer or by coculturing them with fibroblasts on a collagen-coated cell culture dish[67]. In addition, supplementing growth factors into the culture media (such as FGF7[68]) could also improve the colony-forming ability of cells isolated from tissue samples. In addition, over-digestion of tissue using collagenase or trypsin during single cell suspension generation step can result in low to zero colony-forming ability and reduce mammosphere-forming efficiency[31]. In both the assays, care should be taken to incubate the assay plates undisturbed to avoid disruption of colony or sphere structures as they are forming. It is also recommended that users extend the incubation period for primary cells (relative to cell lines) as it might take longer for these cells to form colonies or spheres.

Multiple lines of evidence have demonstrated the critical role of extracellular matrix (ECM)[15,17,69] and stromal components, such as fibroblasts, immune cells, endothelial cells and adipocytes in influencing BCSC functions[15]. Thus, the 3D culture model we describe in this protocol can provide a useful experimental system for helping to recapitulate the *in vivo* tumor microenvironment in an *in vitro* setting. Although the 3D culture system closely resembles the tumor microenvironment in cancer patients, long term maintenance of cells as organoids can be difficult. In addition, optimization of the 3D culture conditions and the ability to accurately investigate self-renewal and differentiation ability of BCSCs is challenging[70]. The efficiency of organoids formed in 3D culture system depends on the growth factors supplemented in the culture media[71]. Absence of key components (for example, ROCK inhibitor) could lead to reduced or no organoid formation[71]. Media should be replenished every 3-4 days to maintain optimal cellular function and the sustainability of the culture. In order to recapitulate *in vivo* conditions and response, it is always important to allow the cells to form organoids prior to any kind of exogenous treatment[72]. Cells derived from patient samples should be giving sufficient time to form organoids, particularly if the objective is the evaluate drug response[72].

While these *in vitro* methods are attractive and accessible experimental tools for characterizing BCSC function, tumor heterogeneity and the effect of tumor microenvironment on BCSC behavior cannot be studied with complete effectiveness. These *in vitro* assays should therefore be complemented with *in vivo* xenograft models whenever feasible in order to further validate experimental findings related to BSCS biology and/or response to novel therapeutics. Different *in vivo* models have been used study BCSC tumorigenicity and metastasis. Ectopic (subcutaneous engraftment) and orthotopic (MFP engraftment) mouse models have been used to generate

breast tumors and assess longitudinal changes in tumor growth over time[50]. Although both *in vivo* injection approaches can be used to study BCSC biology, the native stromal and vasculature-related components of the MFP allow more accurate recapitulation of primary breast tumor progression as observed in patients, and thus MFP injection is preferred[73,74,75]. Finally, the use of immunocompromised mice is required for engraftment of human BCSCs and tumor growth, and this prevents incorporating the role of immune cells in tumorigenesis and metastasis studies[76]. More recently, this limitation has been addressed through the use of humanized mice in which a human immune system is reconstituted via bone marrow transplantation prior to the initiation of xenograft studies[77-79]. However, these models are expensive and technically challenging, and thus are still not commonly used[80].

In summary, here we have provided a protocol for the isolation of human BCSCs from both breast cancer cell lines and patient-derived tumor tissue samples. We have also described *in vitro* and *in vivo* protocols for downstream assays that can be used to study BCSC function, with the ability to be optimized for different breast cancer cell sources and the flexibility to be performed under different experimental conditions. These protocols will be useful for investigators interested in cancer stem cells, breast cancer biology and therapeutic development, with the ultimate goal of improving patient outcomes in the future.

ACKNOWLEDGMENTS:

We thank members of our laboratory for their helpful discussions and support. Our research on breast cancer stem cells and the tumor microenvironment is funded by grants from the Canadian Cancer Research Society Research Institute and the U.S. Army Department of Defense Breast Cancer Program (Grant # BC160912). V.B. is supported by a Western Postdoctoral Fellowship (Western University), and both A.L.A. and V.B. are supported by the Breast Cancer Society of Canada. C.L. is supported by a Vanier Canada Graduate Scholarship from the Government of Canada.

DISCLOSURES:

The authors have nothing to disclose.

REFERENCES:

1 Al-Hajj, M., Wicha, M. S., Benito-Hernandez, A., Morrison, S. J. & Clarke, M. F. Prospective identification of tumorigenic breast cancer cells. *Proceedings of the National Academy of Sciences of the United States of America.* **100** (7), 3983-3988, (2003).

2 Shipitsin, M. *et al.* Molecular definition of breast tumor heterogeneity. *Cancer Cell.* **11** (3), 259-273, (2007).

3 Ginestier, C. *et al.* ALDH1 is a marker of normal and malignant human mammary stem cells and a predictor of poor clinical outcome. *Cell Stem Cell.* **1** (5), 555-567, (2007).

4 Sulaiman, A. *et al.* Dual inhibition of Wnt and Yes-associated protein signaling retards the growth of triple-negative breast cancer in both mesenchymal and epithelial states. *Molecular Oncology.* **12** (4), 423-440, (2018).

5 Debeb, B. G. *et al.* Histone deacetylase inhibitors stimulate dedifferentiation of human breast cancer cells through WNT/β-catenin signaling. *Stem Cells.* **30** (11), 2366-2377,

(2012).
6 Klutzny, S. *et al.* PDE5 inhibition eliminates cancer stem cells via induction of PKA signaling. *Cell Death & Disease.* **9** (2), 192, (2018).
7 DiMeo, T. A. *et al.* A novel lung metastasis signature links Wnt signaling with cancer cell self-renewal and epithelial-mesenchymal transition in basal-like breast cancer. *Cancer Research.* **69** (13), 5364-5373, (2009).
8 Liu, C. C., Prior, J., Piwnica-Worms, D. & Bu, G. LRP6 overexpression defines a class of breast cancer subtype and is a target for therapy. *Proceedings of the National Academy of Sciences of the United States of America.* **107** (11), 5136-5141, (2010).
9 Miller-Kleinhenz, J. *et al.* Dual-targeting Wnt and uPA receptors using peptide conjugated ultra-small nanoparticle drug carriers inhibited cancer stem-cell phenotype in chemo-resistant breast cancer. *Biomaterials.* **152** 47-62, (2018).
10 Mamaeva, V. *et al.* Inhibiting Notch Activity in Breast Cancer Stem Cells by Glucose Functionalized Nanoparticles Carrying γ-secretase Inhibitors. *Molecular Therapy.* **24** (5), 926-936, (2016).
11 Ithimakin, S. *et al.* HER2 drives luminal breast cancer stem cells in the absence of HER2 amplification: implications for efficacy of adjuvant trastuzumab. *Cancer Research.* **73** (5), 1635-1646, (2013).
12 Koike, Y. *et al.* Anti-cell growth and anti-cancer stem cell activities of the non-canonical hedgehog inhibitor GANT61 in triple-negative breast cancer cells. *Breast Cancer.* **24** (5), 683-693, (2017).
13 Sun, Y. *et al.* Estrogen promotes stemness and invasiveness of ER-positive breast cancer cells through Gli1 activation. *Molecular Cancer.* **13** 137, (2014).
14 Colavito, S. A., Zou, M. R., Yan, Q., Nguyen, D. X. & Stern, D. F. Significance of glioma-associated oncogene homolog 1 (GLI1) expression in claudin-low breast cancer and crosstalk with the nuclear factor kappa-light-chain-enhancer of activated B cells (NFκB) pathway. *Breast Cancer Research.* **16** (5), 444, (2014).
15 Bhat, V., Allan, A. L. & Raouf, A. Role of the Microenvironment in Regulating Normal and Cancer Stem Cell Activity: Implications for Breast Cancer Progression and Therapy Response. *Cancers.* **11** (9), (2019).
16 Pio, G. M., Xia, Y., Piaseczny, M. M., Chu, J. E. & Allan, A. L. Soluble bone-derived osteopontin promotes migration and stem-like behavior of breast cancer cells. *PloS One.* **12** (5), e0177640, (2017).
17 Chu, J. E. *et al.* Lung-derived factors mediate breast cancer cell migration through CD44 receptor-ligand interactions in a novel ex vivo system for analysis of organ-specific soluble proteins. *Neoplasia.* **16** (2), 180-191, (2014).
18 McGowan, P. M. *et al.* Notch1 inhibition alters the CD44hi/CD24lo population and reduces the formation of brain metastases from breast cancer. *Molecular Cancer Research.* **9** (7), 834-844, (2011).
19 Mao, J. *et al.* ShRNA targeting Notch1 sensitizes breast cancer stem cell to paclitaxel. *International Journal of Biochemistry and Cell Biology.* **45** (6), 1064-1073, (2013).
20 Duru, N. *et al.* HER2-associated radioresistance of breast cancer stem cells isolated from HER2-negative breast cancer cells. *Clinical Cancer Research.* **18** (24), 6634-6647, (2012).
21 Croker, A. K. & Allan, A. L. Inhibition of aldehyde dehydrogenase (ALDH) activity reduces

chemotherapy and radiation resistance of stem-like ALDHhiCD44$^+$ human breast cancer cells. *Breast Cancer Research and Treatment.* **133** (1), 75-87, (2012).

22 Creighton, C. J. *et al.* Residual breast cancers after conventional therapy display mesenchymal as well as tumor-initiating features. *Proceedings of the National Academy of Sciences of the United States of America.* **106** (33), 13820-13825, (2009).

23 Calcagno, A. M. *et al.* Prolonged drug selection of breast cancer cells and enrichment of cancer stem cell characteristics. *Journal of the National Cancer Institute.* **102** (21), 1637-1652, (2010).

24 Feng, Y. *et al.* Breast cancer development and progression: Risk factors, cancer stem cells, signaling pathways, genomics, and molecular pathogenesis. *Genes and Disease.* **5** (2), 77-106, (2018).

25 Samanta, D., Gilkes, D. M., Chaturvedi, P., Xiang, L. & Semenza, G. L. Hypoxia-inducible factors are required for chemotherapy resistance of breast cancer stem cells. *Proceedings of the National Academy of Sciences of the United States of America.* **111** (50), E5429-5438, (2014).

26 Croker, A. K. *et al.* High aldehyde dehydrogenase and expression of cancer stem cell markers selects for breast cancer cells with enhanced malignant and metastatic ability. *Journal of Cellular and Molecular Medicine.* **13** (8b), 2236-2252, (2009).

27 Morel, A. P. *et al.* Generation of breast cancer stem cells through epithelial-mesenchymal transition. *PloS One.* **3** (8), e2888, (2008).

28 Muntimadugu, E., Kumar, R., Saladi, S., Rafeeqi, T. A. & Khan, W. CD44 targeted chemotherapy for co-eradication of breast cancer stem cells and cancer cells using polymeric nanoparticles of salinomycin and paclitaxel. *Colloids and Surfaces B: Biointerfaces.* **143** 532-546, (2016).

29 Liu, S. *et al.* Breast cancer stem cells transition between epithelial and mesenchymal states reflective of their normal counterparts. *Stem Cell Reports.* **2** (1), 78-91, (2014).

30 Munshi, A., Hobbs, M. & Meyn, R. E. Clonogenic cell survival assay. *Methods in Molecular Medicine.* **110** 21-28, (2005).

31 Shaw, F. L. *et al.* A detailed mammosphere assay protocol for the quantification of breast stem cell activity. *Journal of Mammary Gland Biology and Neoplasia.* **17** (2), 111-117, (2012).

32 Shin, C. S., Kwak, B., Han, B. & Park, K. Development of an in vitro 3D tumor model to study therapeutic efficiency of an anticancer drug. *Molecular Pharmaceutics.* **10** (6), 2167-2175, (2013).

33 Khanna, C. & Hunter, K. Modeling metastasis in vivo. *Carcinogenesis.* **26** (3), 513-523, (2005).

34 Cheon, D. J. & Orsulic, S. Mouse models of cancer. *Annual Review of Pathology.* **6** 95-119, (2011).

35 Lyons, S. K. Advances in imaging mouse tumour models in vivo. *Journal of Pathology.* **205** (2), 194-205, (2005).

36 Margaryan, N. V. *et al.* The Stem Cell Phenotype of Aggressive Breast Cancer Cells. *Cancers.* **11** (3), (2019).

37 Ma, F. *et al.* Enriched CD44(+)/CD24(-) population drives the aggressive phenotypes presented in triple-negative breast cancer (TNBC). *Cancer Letters.* **353** (2), 153-159,

(2014).
38 Chatterjee, S. *et al.* Paracrine Crosstalk between Fibroblasts and ER(+) Breast Cancer Cells Creates an IL1β-Enriched Niche that Promotes Tumor Growth. *iScience.* **19** 388-401, (2019).
39 Phan-Lai, V. *et al.* Three-dimensional scaffolds to evaluate tumor associated fibroblast-mediated suppression of breast tumor specific T cells. *Biomacromolecules.* **14** (5), 1330-1337, (2013).
40 O'Brien, C. A., Kreso, A. & Jamieson, C. H. Cancer stem cells and self-renewal. *Clinical Cancer Research.* **16** (12), 3113-3120, (2010).
41 Hu, Y. & Smyth, G. K. ELDA: extreme limiting dilution analysis for comparing depleted and enriched populations in stem cell and other assays. *Journal of Immunological Methods.* **347** (1-2), 70-78, (2009).
42 Stewart, J. M. *et al.* Phenotypic heterogeneity and instability of human ovarian tumor-initiating cells. *Proceedings of the National Academy of Sciences of the United States of America.* **108** (16), 6468-6473, (2011).
43 Abraham, B. K. *et al.* Prevalence of CD44+/CD24-/low cells in breast cancer may not be associated with clinical outcome but may favor distant metastasis. *Clinical Cancer Research.* **11** (3), 1154-1159, (2005).
44 Balic, M. *et al.* Most early disseminated cancer cells detected in bone marrow of breast cancer patients have a putative breast cancer stem cell phenotype. *Clinical Cancer Research.* **12** (19), 5615-5621, (2006).
45 Charafe-Jauffret, E. *et al.* Aldehyde dehydrogenase 1-positive cancer stem cells mediate metastasis and poor clinical outcome in inflammatory breast cancer. *Clinical Cancer Research.* **16** (1), 45-55, (2010).
46 Marcato, P. *et al.* Aldehyde dehydrogenase activity of breast cancer stem cells is primarily due to isoform ALDH1A3 and its expression is predictive of metastasis. *Stem Cells.* **29** (1), 32-45, (2011).
47 Lacerda, L., Pusztai, L. & Woodward, W. A. The role of tumor initiating cells in drug resistance of breast cancer: Implications for future therapeutic approaches. *Drug Resistance Updates.* **13** (4-5), 99-108, (2010).
48 Liu, S. & Wicha, M. S. Targeting breast cancer stem cells. *Journal of Clinical Oncology.* **28** (25), 4006-4012, (2010).
49 D'Angelo, R. C. *et al.* Notch reporter activity in breast cancer cell lines identifies a subset of cells with stem cell activity. *Molecular Cancer Therapeutics.* **14** (3), 779-787, (2015).
50 Neve, R. M. *et al.* A collection of breast cancer cell lines for the study of functionally distinct cancer subtypes. *Cancer Cell.* **10** (6), 515-527, (2006).
51 Forozan, F. *et al.* Comparative genomic hybridization analysis of 38 breast cancer cell lines: a basis for interpreting complementary DNA microarray data. *Cancer Research.* **60** (16), 4519-4525, (2000).
52 Lanier, L. L. Just the FACS. *Journal of Immunology.* **193** (5), 2043-2044, (2014).
53 Ibrahim, S. F. & van den Engh, G. Flow cytometry and cell sorting. *Advances in Biochemical Engineering/Biotechnology.* **106** 19-39, (2007).
54 Shapiro, H. M. Flow Cytometry: The Glass Is Half Full. *Methods in Molecular Biology.* **1678** 1-10, (2018).

55 Tsuji, K. *et al.* Effects of Different Cell-Detaching Methods on the Viability and Cell Surface Antigen Expression of Synovial Mesenchymal Stem Cells. *Cell Transplantation.* **26** (6), 1089-1102, (2017).
56 Sun, C. *et al.* Immunomagnetic separation of tumor initiating cells by screening two surface markers. *Scientific Reports.* **7** 40632, (2017).
57 Rodríguez, C. E. *et al.* Breast cancer stem cells are involved in Trastuzumab resistance through the HER2 modulation in 3D culture. *Journal of Cellular Biochemistry.* **119** (2), 1381-1391, (2018).
58 Kim, D. W. & Cho, J. Y. NQO1 is Required for β-Lapachone-Mediated Downregulation of Breast-Cancer Stem-Cell Activity. *International Journal of Molecular Sciences.* **19** (12), (2018).
59 Xu, L. Z. *et al.* p62/SQSTM1 enhances breast cancer stem-like properties by stabilizing MYC mRNA. *Oncogene.* **36** (3), 304-317, (2017).
60 Huang, X. *et al.* Breast cancer stem cell selectivity of synthetic nanomolar-active salinomycin analogs. *BMC Cancer.* **16** 145, (2016).
61 Liu, T. J. *et al.* CD133+ cells with cancer stem cell characteristics associates with vasculogenic mimicry in triple-negative breast cancer. *Oncogene.* **32** (5), 544-553, (2013).
62 Velasco-Velázquez, M. A., Popov, V. M., Lisanti, M. P. & Pestell, R. G. The role of breast cancer stem cells in metastasis and therapeutic implications. *American Journal of Pathology.* **179** (1), 2-11, (2011).
63 Palomeras, S., Ruiz-Martínez, S. & Puig, T. Targeting Breast Cancer Stem Cells to Overcome Treatment Resistance. *Molecules.* **23** (9), (2018).
64 McClements, L. *et al.* Targeting treatment-resistant breast cancer stem cells with FKBPL and its peptide derivative, AD-01, via the CD44 pathway. *Clinical Cancer Research.* **19** (14), 3881-3893, (2013).
65 Berger, D. P., Henss, H., Winterhalter, B. R. & Fiebig, H. H. The clonogenic assay with human tumor xenografts: evaluation, predictive value and application for drug screening. *Annals of Oncology.* **1** (5), 333-341, (1990).
66 Tian, J. *et al.* Dasatinib sensitises triple negative breast cancer cells to chemotherapy by targeting breast cancer stem cells. *British Journal of Cancer.* **119** (12), 1495-1507, (2018).
67 Samoszuk, M., Tan, J. & Chorn, G. Clonogenic growth of human breast cancer cells co-cultured in direct contact with serum-activated fibroblasts. *Breast Cancer Research.* **7** (3), R274-283, (2005).
68 Palmieri, C. *et al.* Fibroblast growth factor 7, secreted by breast fibroblasts, is an interleukin-1beta-induced paracrine growth factor for human breast cells. *Journal of Endocrinology.* **177** (1), 65-81, (2003).
69 Bourguignon, L. Y., Peyrollier, K., Xia, W. & Gilad, E. Hyaluronan-CD44 interaction activates stem cell marker Nanog, Stat-3-mediated MDR1 gene expression, and ankyrin-regulated multidrug efflux in breast and ovarian tumor cells. *Journal of Biological Chemistry.* **283** (25), 17635-17651, (2008).
70 Yin, X. *et al.* Engineering Stem Cell Organoids. *Cell Stem Cell.* **18** (1), 25-38, (2016).
71 Sachs, N. *et al.* A Living Biobank of Breast Cancer Organoids Captures Disease Heterogeneity. *Cell.* **172** (1-2), 373-386.e310, (2018).
72 Kim, M. *et al.* Patient-derived lung cancer organoids as in vitro cancer models for

therapeutic screening. *Nature Communications* **10** (1), 3991, (2019).
73 Okano, M. *et al.* Orthotopic Implantation Achieves Better Engraftment and Faster Growth Than Subcutaneous Implantation in Breast Cancer Patient-Derived Xenografts. *Journal of Mammary Gland Biology and Neoplasia.* **25** (1), 27-36, (2020).
74 Zhang, Y. *et al.* Establishment of a murine breast tumor model by subcutaneous or orthotopic implantation. *Oncology Letters.* **15** (5), 6233-6240, (2018).
75 Zhang, W. *et al.* Comparative Study of Subcutaneous and Orthotopic Mouse Models of Prostate Cancer: Vascular Perfusion, Vasculature Density, Hypoxic Burden and BB2r-Targeting Efficacy. *Scientific Reports.* **9** (1), 11117, (2019).
76 Kim, R., Emi, M. & Tanabe, K. Cancer immunoediting from immune surveillance to immune escape. *Immunology.* **121** (1), 1-14, (2007).
77 Rosato, R. R. *et al.* Evaluation of anti-PD-1-based therapy against triple-negative breast cancer patient-derived xenograft tumors engrafted in humanized mouse models. *Breast Cancer Research.* **20** (1), 108, (2018).
78 Choi, Y. *et al.* Studying cancer immunotherapy using patient-derived xenografts (PDXs) in humanized mice. *Experimental and Molecular Medicine.* **50** (8), 99, (2018).
79 Meraz, I. M. *et al.* An Improved Patient-Derived Xenograft Humanized Mouse Model for Evaluation of Lung Cancer Immune Responses. *Cancer Immunology Research* **7** (8), 1267-1279, (2019).
80 Wege, A. K. Humanized Mouse Models for the Preclinical Assessment of Cancer Immunotherapy. *Biodrugs.* **32** (3), 245-266, (2018).

A

Harvest breast cancer cells from cell cultures/
Collect patient-derived surgical or biopsy samples

↓

Generate single cell suspension from cell lines/tissue samples

↓

Incubate cells with ALDH substrate , anti-CD44 & anti-CD24 antibodies

↓

Sort $ALDH^{high}CD44^{+}CD24^{-}$ and $ALDH^{lo}CD44^{-}CD24^{-}$ cells

↓

Functional assays

↙ ↘

In vitro assays
Colony forming assay,
mammosphere assay & 3D culture

In vivo xenograft model

B

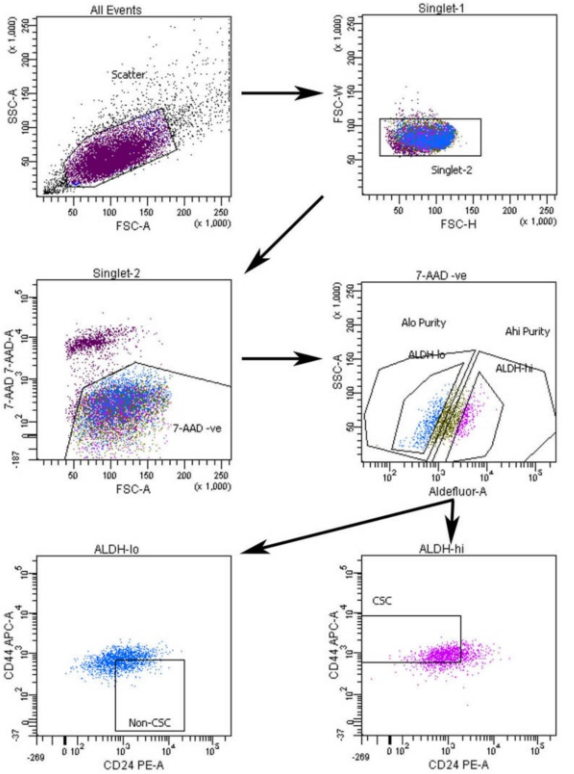

A

MDA-MB-231

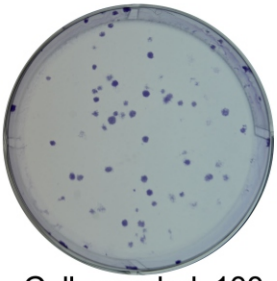

Cells seeded: 100

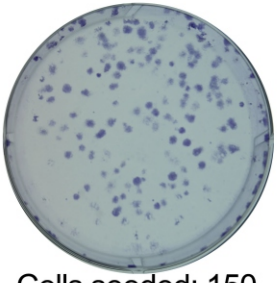

Cells seeded: 150

B

MCF7

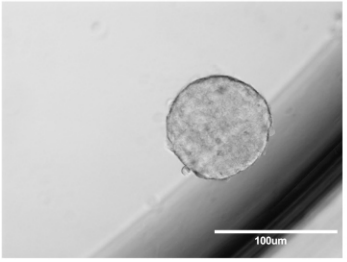

SUM159

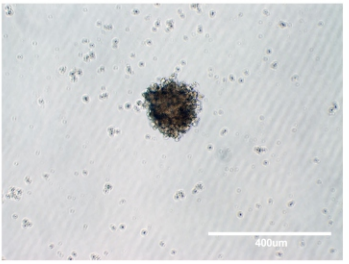

MDA-MB-468

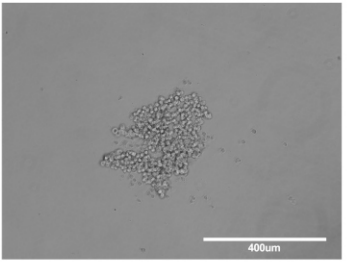

LRCP17

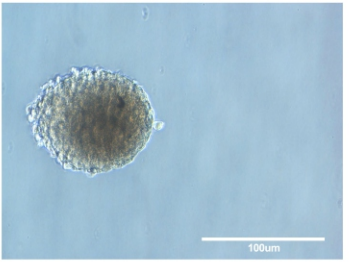

C

MCF7

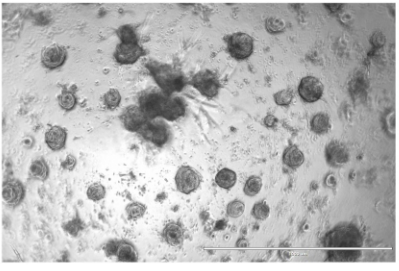

MDA-MB-231

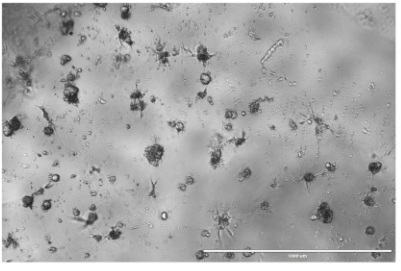

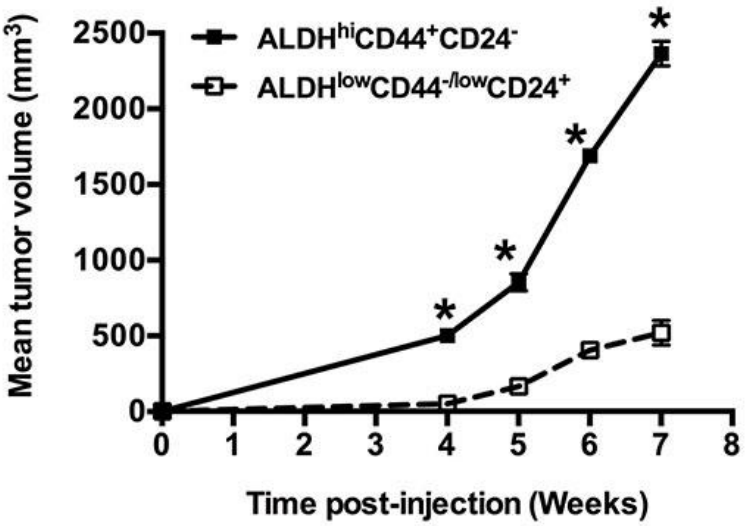
Mean tumor volume (mm3)
2500
2000
1500
1000
500
0
ALDHhiCD44+CD24-
ALDHlowCD44-/lowCD24+
*
*
*
*
0
1
2
3
4
5
6
7
8
Time post-injection (Weeks)